

Sedimentological, palynological and geochemical studies of the terrestrial Triassic–Jurassic boundary in northwestern Poland

GRZEGORZ PIENKOWSKI*†, GRZEGORZ NIEDŹWIEDZKI‡ &
MARTA WAKSMUNDZKA*

*Polish Geological Institute – National Research Institute, ul. Rakowiecka 4, 00-975 Warszawa, Poland
‡Department of Paleobiology and Evolution, Faculty of Biology, University of Warsaw, ul. S. Banacha 2,
PL-02-097 Warszawa, Poland

(Received 14 May 2010; accepted 8 March 2011; first published online 12 September 2011)

Abstract – The Kamień Pomorski IG-1 borehole (Pomerania, NW Poland) yields a profile through the Triassic–Jurassic (T–J) transition in continental deposits. An integrated study of the sedimentology, sequence stratigraphy, palynology, biostratigraphy and geochemistry of these deposits has been carried out on the boundary interval, which represents a time of major environmental change. Two lithological units within the transitional section are distinguished: the Lower–Middle Rhaetian Wielichowo Beds of alluvial plain facies, which shows evidence of a semi-arid climate, and the Upper Rhaetian to Lower Hettangian Zagaje Formation, lying above a marked erosional sequence boundary, composed of mudstone–claystone and sandstone deposited in a fluvial–lacustrine environment. Carbon isotope values obtained from palynomaceral separates, and thus reflecting isotopic changes in atmospheric CO₂, show significant fluctuations through the Rhaetian; the most conspicuous negative $\delta^{13}\text{C}_{\text{org}}$ excursion is correlated with the Rhaetian ‘initial’ excursion and shows two sub-peaks, pointing to short-term carbon-cycle disturbances of lesser magnitude. Above the ‘initial’ negative excursion, there is a positive excursion followed again by more negative values, representing subordinate fluctuation within a positive excursion and is correlated with the T–J boundary. Seventy-two miospore taxa have been determined from the studied T–J transitional section. Two major palynological assemblages have been distinguished: the lower one, typically Rhaetian, named the *Cingulizonates rhaeticus–Limbosporites lundblandii* association, which corresponds to the *Rhaetipollis–Ricciisporites* (= *Rhaetipollis–Limbosporites*) Zone; and the upper one, typically Hettangian, named the *Conbaculatisporites mesozoicus–Dictyophyllidites mortoni–Cerebropollenites thiergartii* association (with the age-diagnostic pollen *C. thiergartii*), which corresponds to the *Pinuspollenites–Trachysporites* (= *Trachysporites–Heliosporites*) Zone. The T–J palynofloral turnover occurred in a humid period and is more conspicuous than palynofloral changes observed in Greenland, the Tethyan domain or other parts of NE Europe. The osmium isotope system is studied herein for the first time from T–J continental deposits and shows marked disturbances similar to those measured in marine deposits and attributed to volcanic fallout. Carbon and osmium isotope correlation and coeval increase in polycyclic aromatic hydrocarbon (PAH) content and darkening of miospores confirm that eruptions of the Central Atlantic Magmatic Province (CAMP) contributed to the perturbances in climate and crisis in the terrestrial biosphere. A series of periodical atmospheric loading by CO₂, CH₄ or alternatively by SO₂, sulphate aerosols and toxic compounds is inferred to have caused a series of rapid climatic reversals, directly influencing the ecosystem and causing the Triassic floral crisis. A floral turnover period commenced at the ‘initial’ $\delta^{13}\text{C}$ excursion, with the onset of CAMP volcanism. Obtained values of initial ¹⁸⁷Os/¹⁸⁶Os between 2.905 and 4.873 and very low iridium content (about 5 ppt) lend no support to a role for an extraterrestrial impact at the T–J boundary event. The position of sequence boundaries (emergence surfaces) and other isotope excursions allow reliable correlation with marine profiles, including St Audrie’s Bay (UK), Csövár (Hungary) and the GSSP profile at Kuhjoch (Austria).

Keywords: Triassic–Jurassic boundary, carbon isotopes, osmium isotopes, palynofloral turnover, global correlation.

1. Introduction

The Triassic–Jurassic (T–J) boundary is associated with a one of the five largest mass extinction events in the Phanerozoic, and appears to coincide with volcanism of the Central Atlantic Magmatic Province (CAMP) (Pálfy, 2003; Marzoli *et al.* 2004; Tanner,

Lucas & Chapman, 2004; Cirilli *et al.* 2009). Emplacement of the GSSP for the base of the Hettangian and hence the T–J boundary at the first occurrence of the ammonite *Psiloceras spelae* in the Kuhjoch section in Austria (Hillebrandt *et al.* 2007) was accepted by votes within the Triassic–Jurassic Boundary Working Group and the International Subcommittee on Jurassic Stratigraphy (Morton, 2008a,b; Morton, Warrington & Bloos, 2008) and finally (16 April 2010) ratified by

†Author for correspondence: grzegorz.pienkowski@pgi.gov.pl

the Executive Committee of the International Union of Geological Sciences. At Kuhjoch, the first occurrence of *Psiloceras spelae* is found ~ 6 m above a negative carbon isotope excursion and is also associated with palynofloral turnover observed at Kuhjoch and in adjacent sections (Bonis, Kürschner & Krystyn, 2009). Study of the T–J transition has gained considerable impetus in recent years (e.g. McElwain, Beerling & Woodward, 1999; McElwain *et al.* 2007; Olsen *et al.* 2002; Hesselbo *et al.* 2002; Hesselbo, Robinson & Surlyk, 2004; Hesselbo, McRoberts & Pálffy, 2007; Hounslow, Posen & Warrington, 2004; Guex *et al.* 2004; Marzoli *et al.* 2004; Galli *et al.* 2005; Cirilli *et al.* 2009; Muttoni *et al.* 2010). Carbon isotope values show significant fluctuations through Rhaetian–Hettangian time, with two conspicuous negative $\delta^{13}\text{C}_{\text{org}}$ excursions. There is an ‘increasingly replicated pattern of an abrupt “initial” negative excursion, closely followed by an extended “main” isotope excursion’ (Hesselbo, McRoberts & Pálffy, 2007) across the T–J boundary. Specifically, above the ‘initial’ negative excursion, there is a positive excursion followed again by more negative values, representing subordinate fluctuation within a positive excursion. The subordinate negative peak within the positive excursion is correlated with the T–J boundary (Korte *et al.* 2009). Thus, the studies of the carbon-cycle disturbances are very useful in discussions on the placement of the T–J boundary and its global correlation (e.g. Pálffy *et al.* 2001; Galli *et al.* 2005; Hesselbo, McRoberts & Pálffy, 2007; Hillebrandt *et al.* 2007; Korte *et al.* 2009).

Global anoxic events, regression, primary productivity crash, methane hydrate release and rapid global warming, and oceanic productivity crises have all figured in recently proposed kill mechanisms (Hallam & Wignall, 1997, 1999; Pálffy *et al.* 2001; Pálffy, Smith & Mortensen, 2000; Hesselbo *et al.* 2002; Hesselbo, McRoberts & Pálffy, 2007; Ward *et al.* 2001, 2004; Galli *et al.* 2005; McElwain, Beerling & Woodward, 1999; McElwain *et al.* 2007). The search for trigger mechanisms has focused also on the possibility of rare astronomical-geological events such as a bolide impact (Olsen *et al.* 2002; Simms, 2007). The biostratigraphy and carbon isotope profiles across the T–J boundary in Canada (Ward *et al.* 2001), Hungary (Pálffy *et al.* 2001, 2007; Haas & Tardy-Filác, 2004), United Kingdom (Hesselbo *et al.* 2002; Hesselbo, Robinson & Surlyk, 2004), Nevada, USA (Guex *et al.* 2004; Ward *et al.* 2007), Italy (Galli *et al.* 2005) and Austria (Kürschner, Bonis & Krystyn, 2007; Hillebrandt *et al.* 2007) can be correlated and show a regression–transgression couplet coincident with changes in the carbon isotope curve. It is not clear whether these sea-level changes were eustatic or, alternatively, epeirogenic and linked to the CAMP volcanism (Hallam, 1997; Hallam & Wignall, 1999).

Carbon isotope trends in particular have proved useful in evaluation of palaeoenvironmental changes during biotic crises. Perturbations in the Earth’s carbon cycle represent geologically instantaneous events, are

of a global scale and can potentially be observed in marine and continental settings in a variety of facies (Kump & Arthur, 1999; Beerling & Berner, 2002; Korte *et al.* 2009; Deenen *et al.* 2010; Whiteside *et al.* 2010). Resolution of extinction timing and the recognition of an ecological selectivity to the extinctions have also helped clarify the nature of the crisis (McRoberts & Newton, 1995; Sephton *et al.* 2002; Ward *et al.* 2001, 2004; McElwain *et al.* 2007; McElwain, Beerling & Woodward, 1999; McElwain, Wagner & Hesselbo, 2009; Deenen *et al.* 2010; Whiteside *et al.* 2010). In contrast, other authors have questioned whether the boundary can even be characterized unequivocally as a mass extinction. Hallam (2002) has argued that the tempo of extinction was gradual rather than catastrophically rapid, whereas others (Tanner, Lucas & Chapman, 2004) suggest that most of the apparent biodiversity losses across the T–J boundary are due to biases or artefacts of sampling or poor stratigraphical control.

The present paper attempts to address these issues using a multidisciplinary dataset gathered from a T–J boundary section in continental deposits from a cored borehole, which was drilled near Kamień Pomorski in the Pomerania region in northwestern Poland. Palaeontological and geological observations, including palynology and sedimentology, are compared with geochemical data, including carbon isotopes, osmium and rhenium isotopes, and iridium content.

In this paper, in an attempt to better constrain our understanding of the causes and consequences of one of the five greatest extinction events in Earth history, we: (1) document the miospore biostratigraphic framework; (2) present an analysis of the vegetation change spanning the T–J extinction event from a census chosen palynofloral dataset of more than 5000 miospores; (3) report analyses that establish a carbon isotope correlation with other profiles and sea-level changes across the T–J boundary; (4) report first ever analyses of the Os and Re isotope system across the T–J boundary in continental deposits.

2. Geological and palaeogeographical setting

Two boreholes from Pomerania, northwestern Poland (Kamień Pomorski IG-1 and Mechowo IG-1, located 25 km to the SE) (Dadlez, 1972), have yielded core material from the T–J transition in continental deposits (Fig. 1). Recovery of core in the Kamień Pomorski borehole was about 42 % in the Rhaetian and Hettangian and, fortunately, the core was recovered from the most important parts of the profile (including the T–J boundary interval). In Mechowo IG-1 the core recovery was above 90 %, but the Rhaetian–Hettangian boundary occurs within a thick sandstone succession of fluvial origin and this boundary is determined only based on sparse occurrences of megaspores (*Trileites pinguis* assemblage, Rhaetian, and *Nathorstisporites hopliticus* assemblage, Hettangian, see Marcinkiewicz, 1971). In Pomerania, the Rhaetian sediments show

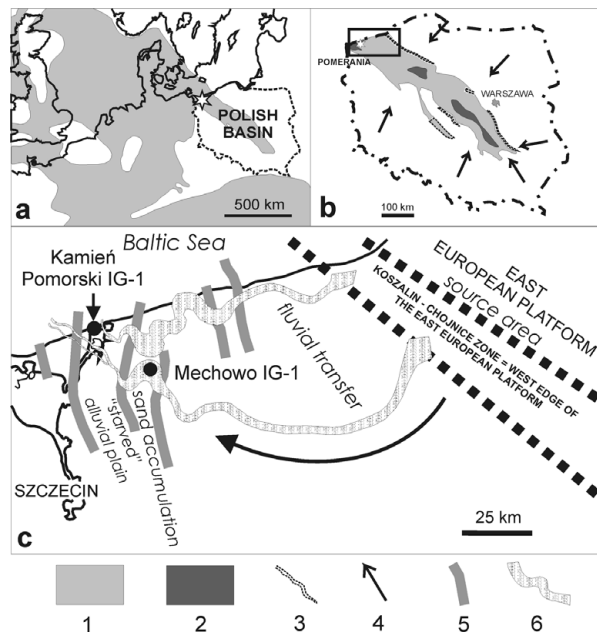


Figure 1. Palaeogeography and location of study area: (a) Palaeogeographic map of the Early Jurassic basins in Europe with location of Kamień Pomorski; (b) General palaeogeographic map of the Early Hettangian in Poland: 1 – alluvial plain, 2 – lacustrine, 3 – main fracture zones, 4 – main sediment transport directions; (c) Location of boreholes Kamień Pomorski IG-1 and Mechowo IG-1 and the general palaeogeography of the Late Rhaetian–earliest Hettangian alluvial plain deposits in Pomerania (framed section of the map in (b)): 5 – syn-sedimentary faults, 6 – fluvial channels (after Pieńkowski, 2004).

conspicuous bi-partite development (Fig. 2). The lower part, belonging to the Lower–Middle Rhaetian Wielichowo Beds, is represented by brownish or variegated mudstone, with rare, scattered calcium-carbonate concretions. In places, poorly preserved, oxidized rootlets with iron-oxide rhizoconcretion mottles occur. These features are indicative of a climate characterized by seasonal precipitation in which evapotranspiration exceeded precipitation, and where the water table fluctuated during the year (a dry inland basin of playa character in a semi-arid, seasonal climate).

The Upper Rhaetian (lowermost Zagaje Formation *sensu* Pieńkowski, 2004) commences with sandstones resting on a marked erosional boundary (698 m in Kamień Pomorski borehole), correlated with the sequence boundary, which is probably concomitant with the Rhaetian lowstand, inferred to be one of the lowest in the Phanerozoic (Hallam, 1997). This sequence boundary can be correlated with emergence surfaces within the Westbury Fm, occurring both in the St Audrie's (Hesselbo *et al.* 2002) and Larne (Simms & Jarem, 2006) sections, and a lowstand (correlative with a sequence boundary) at Kuhjoch, located at the top of Koessen Fm (Hillebrandt *et al.* 2007) and in Csövár (Pálffy *et al.* 2001, 2007). Lithologically these beds comprise grey sandstone and mudstone with coalified rootlets. Carbonate concretions are replaced by sideritic ones, and their oxidization is responsible for red staining of the mudstones, although in places

the red colours in mudstones are also primary. The Late Rhaetian climate must have been wetter than in the Early–Middle Rhaetian, although drier periods still occurred. In Mechowo IG-1, thick sandstone packages of fluvial origin make the Upper Rhaetian–Lower Hettangian Zagaje Formation and are much thicker than in the Kamień Pomorski IG-1 borehole, where finer sediments of floodplain, lacustrine and crevasse splay facies prevail (Fig. 2). This indicates a substantial decrease in depositional energy of the alluvial palaeoenvironment to the west and northwest, which reflects both palaeoslope (Mechowo was closer to the sedimentary source area, situated behind the major Kozalin–Chojnice dislocation zone, in the East European Platform) and local tectonic factors (Fig. 1). In Rhaetian and Jurassic times, the studied area was affected by a number of N–S-trending faults, grabens and half-grabens (Dadlez, 1969; Dadlez *et al.* 1998). These syn-sedimentary faults and grabens acted as traps for sandy sediments; therefore, the deposition of coarser sediments took place largely east of Kamień Pomorski, around the Mechowo area. A steep palaeoslope favoured erosion at the Kozalin–Chojnice dislocation zone and then fast fluvial transfer to the east, with the dominance of straight- to low-sinuosity channels. Further to the west, the river system entered the zone of faults and grabens in the western part of the area studied. This was the area of the Mechowo IG-1 borehole, characterized by fast accumulation of sand and the dominance of high-sinuosity, meandering fluvial channels (Figs 1, 2; see amalgamated meandering channel deposits). Still further to the west and northwest, channel energy decreased and only a minor part of the sandy sediment could be transported ('starved' alluvial plain, likely of meandering-anastomosing character, with high-sinuosity channels). As a result, muddy overbank deposits dominate in the Kamień Pomorski IG-1 profile (Figs 1, 2). Climate became wetter, as indicated by palaeosols with numerous coalified plant roots and numerous well-preserved, coalified, drifted floral remains. During that period, the region was gradually transforming into wetlands.

At the top of the Rhaetian deposits, the second sequence boundary occurs (678.4 m). This boundary is marked by regional erosion in the sedimentary basin of Poland, and also in some localities in Sweden (Lindström & Erlström, 2006) and Western Europe, but owing to a local tectonic regime, this erosion in Kamień Pomorski was rather less; fine-grained sandstone above the erosional boundary does not contain coarser grains or mud clasts, and bedding at the bottom of the sandstone is characteristic of a rhythmic, lower flow regime (Fig. 2; depth 678.4 m). This is an exceptional case in the Early Jurassic Polish Basin, because commonly the Rhaetian deposits are truncated from the top by erosion, at this regional sequence boundary, often merged with the lower sequence boundaries between Middle and Upper Rhaetian and between Rhaetian and Norian deposits (Pieńkowski,

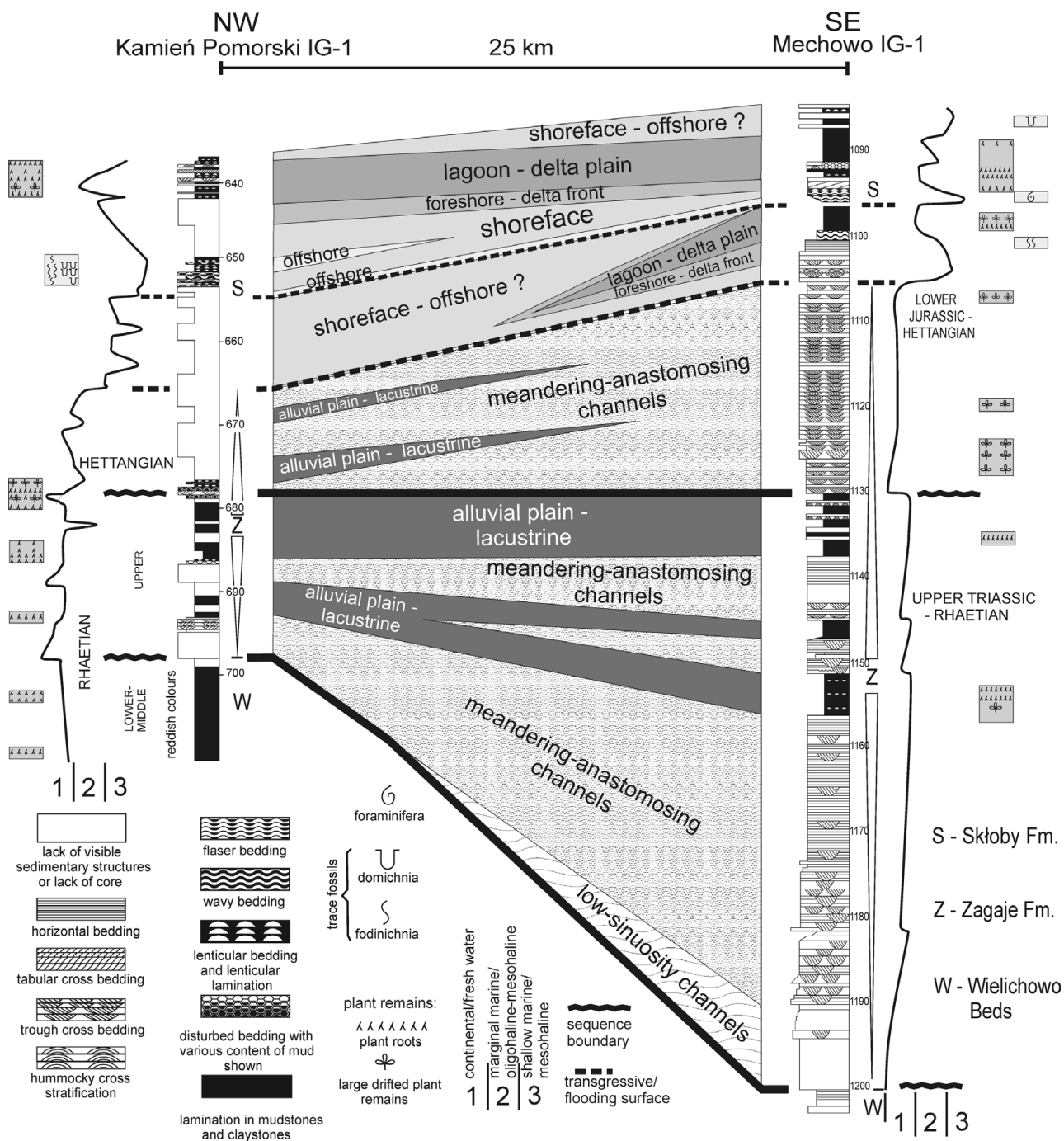


Figure 2. Lithological cross-section of the Upper Rhaetian–Lower Hettangian alluvial deposits in Western Pomerania between Kamień Pomorski and Mechowo; note decrease in depositional energy towards the NW and resulting decrease in thickness of fluvial channel sediments.

2004). Nevertheless, possible erosion at the second sequence boundary at Kamień Pomorski should be also taken into consideration.

Subsequent Early Jurassic sedimentation in Poland and in Pomerania has been characterized in detail by Pieńkowski (2004). The lowermost part of the Hettangian deposits in the Mechowo IG-1 borehole (Figs 2, 3) contains the Hettangian to Early Sinemurian megaspore *Nathorstisporites hopliticus* (Marcinkiewicz, 1971) and is developed as medium-grained, trough cross-bedded sandstone representing entirely the alluvial (meandering channel–point bar)

depositional subsystem. In Kamień Pomorski IG-1 (depth 665.5 to 678.4 m), the grain size of sediments is significantly finer and overbank subsystems (floodplain, lacustrine and crevasse splays) dominate. Earliest Hettangian alluvial deposition was a continuation of Rhaetian deposition, and therefore both Upper Rhaetian and lowermost Hettangian alluvial deposits are assigned to the same lithostratigraphic unit, the Zagaje Formation (Pieńkowski, 2004).

At a depth of 1105 m at Mechowo IG-1, a major Hettangian transgressive surface is recorded (Pieńkowski, 2004). At Kamień Pomorski, this transgressive surface

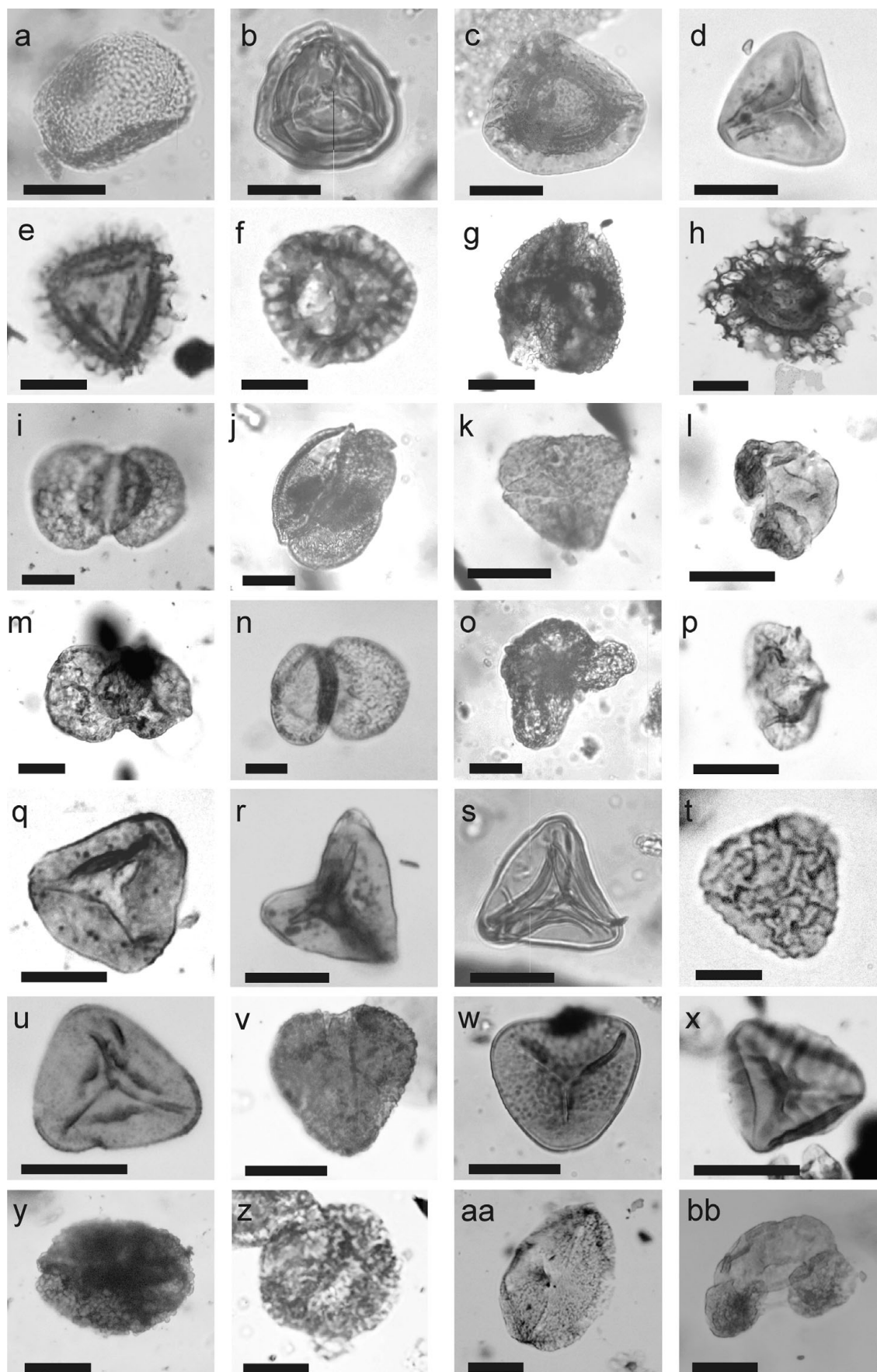


Figure 4. Selected characteristic miospores of the Triassic–Jurassic boundary section in Kamiień Pomorski (compare with Fig. 3). **Triassic taxa: spores:** (a) *Baculatisporites comaumensis* (Cookson) Potonie, depth 680.7 m; (b, c) *Cingulizonates rhaeticus* (Reinhardt) Schulz: (b) 677.5 m, (c) 703.2 m; (d) *Deltoidospora toralis* (Leschik) Lund, 699.3 m; (e, f) *Limbosporites lundblandii* Nilsson: (e) 703.2 m, (f) 678.6 m; (g) *Ricciisporites tuberculatus* Lundblad (tetrad, transitional T–J form), 678.6 m; (h) *Semiretisporis*

occurs within the uncored section and, based on wire log correlation, is tentatively placed at a depth of 665 m. The overlying sediments both in Mechow IG-1 and Kamień Pomorski IG-1 are characterized by mudstone, heterolithic and medium-grained to fine-grained sandstone with dolomitic cement, containing horizontal bedding, trough cross-bedding and hummocky cross-stratification. This complex is divided into several parasequences, identified as being deposited in the shoreface-foreshore-barrier depositional subsystems, and is assigned to the Skłoby Formation (Pieńkowski, 2004). The flooding surfaces are identified where dark, lagoonal deposits containing plant roots in the uppermost part are overlain by wavy- and flaser dolomitic heteroliths with microhummocky cross-lamination containing foraminifera and acritarchs. Progradation in each parasequence is represented by a succession of nearshore/barrier and lagoonal depositional systems, ending with marshy deposits with palaeosols and thin coal seams. Flooding events were associated with elevation of the water table and changes in O₂ conditions in the sediment, resulting in pyritization of deeper plant roots.

3. Material and methods

3.a. Palynology

Fifteen rock samples from the Kamień Pomorski IG-1 core were taken for quantitative palynological analysis; 12 of them yielded palynomorphs (Figs 3, 4). Samples of different weights (about 20–100 g) were dried and crushed into small fragments. Subsequently, samples were treated twice alternately with cold HCl (30%) and cold HF (38%) in order to remove the carbonate and silicate minerals. The residue was washed with water until a neutral pH was reached. ZnCl₂ was applied to separate organic and inorganic residue (e.g. pyrite). Slide preparations, three of each sample, were made in glycerine jelly. Permanent slides are stored in the collection of the Department of Regional Geology, Economic Geology and Geophysics, Polish Geological Institute, Poland.

Palynological terminology used in this paper includes the following terms: ‘floral remains’ – used here for large floral (macrofloral) remains; ‘palynomaceral’ (= kerogen) – all the HF-resistant organic material; ‘phytoclasts’ – all microscopic remains of vegetative plant tissue (wood, cuticle, etc.) and charcoal; ‘palynomorphs’ – here, microscopic, single-celled,

reproductive bodies built of sporopollenin, such as megaspores, spores, pollen grains plus Acritarcha; ‘spore’ – smaller reproductive structures of plants adapted for dispersion; ‘pollen grain’ – a structure produced by plants containing the male gamete to be used in reproduction, commonly with air sacs; ‘miospores’ – spores and pollen grains together; ‘megaspore’ – a type of large spore coming from heterosporous plants; ‘palynofloral’ – here everything regarding miospores and megaspores.

3.b. Carbon isotope analysis

A set of 24 samples from the Kamień Pomorski IG-1 borehole (Fig. 6) was prepared for carbon isotope analysis of bulk sedimentary organic matter, representing mostly phytoclasts, including charcoal. About 30–50 g of sediment were crushed and treated twice with cold HCl (30%) and cold HF (38%) in order to remove the carbonate and the silicate. The residues were washed with water until a neutral pH was achieved and subsequently freeze dried. Phytoclasts were separated manually under the binocular microscope from palynomorphs, and only phytoclast separates were taken for the carbon isotope analysis. Additionally, charcoal was separated in one sample and carbon isotope ratios obtained both from charcoal and other phytoclasts. The results were almost identical, pointing to the lack of isotopic differentiation between charcoal and other phytoclasts. The carbon isotope ratios were measured on homogenized samples by a Carlo-Erba 1110 elemental analyzer connected online to a Thermo Finnigan Delta Plus mass spectrometer. All carbon isotope values are reported in the conventional δ -notation in per mil relative to VPDB (Vienna Pee Dee Belemnite). Accuracy and reproducibility of the analyses were checked by replicate analyses of international standard USGS 40. Analytical precision: mean (μ) = –26.18 and one standard deviation (σ) = 0.06.

It should be noted that 24 samples spanning > 60 m of section is a relatively small number of carbon isotopic data on which to report. However, 35 m of that 60 m section were not cored at all. We sampled the remaining 25 m as densely as possible (considering also the preservation of the core), and actually the average density of sampling in the cored profile is close to one sample per 1 m, although sampling density is not equal, also due to core preservation and lithology (only mudstones yielded enough palynomaceral material).

gothae Reinhardt, 678.6 m; **pollen grains:** (i) *Angustisulcites klausii* Freudenthal, 680.7 m; (j) *Brachysaccus neomundanus f. minor* (Leschik) Lund, 703.2 m; (k) *Microreticulatisporites fuscus* (Nilsson) Morbey, 691 m; (l) *Minutosaccus potonie* Mädlar, 699.3 m; (m) *Platysaccus niger* Mädlar, 680.7 m; (n) *Platysaccus nitidus* Pastuch, 703.2 m; (o) *Schizosaccus keuperi* Mädlar, 691 m; (p) *Vitreisporites pallidus* (Reissinger) Nilsson, 686 m (transitional T–J form). **Jurassic taxa: spores:** (q) *Conbaculatisporites mesozoicus* Klaus, 642.1 m; (r, s) *Dictyophyllidites mortoni* (de Jersey) Playford & Dettmann: (r) 677.5 m, (s) 650.3 m; (t) *Lycopodiumsporites semimuris* Danze-Corsin & Laveine, 676.8 m; (u, v) *Trachysporites asper* Nilsson, 642.1 m; (w) *Trachysporites fuscus* Nilsson, 642.1 m; (x) *Zebbrasporites interscriptus* (Thiergart) Klaus, 650.3 m; **pollen grains:** (y, z) *Cerebropollenites thiergartii* Schulz: (y) 677.5 m, (z) 650.3 m; (aa) *Ovalipolis ovalis* Krutzsch, 678.6 m (transitional T–J form); (bb) *Pinuspollenites minimus* (Couper) Kemp, 642.1 m (transitional T–J form). Scale bar = 25 μ m.

3.c. Osmium and rhenium isotope analyses and iridium content

Analyses of osmium, iridium and rhenium content, as well as analyses of the following isotopes, ¹⁸⁶Os, ¹⁸⁷Os, ¹⁸⁸Os, ¹⁹²Os and ¹⁸⁷Re, were carried out on nine samples (Table 1; Fig. 8). The analytical procedure used here followed that described in detail by Brauns (2001). In brief, all samples (0.2–0.75 g) were weighed into pre-spiked Carius tubes and dissolved and equilibrated using inverse *aqua regia* in an oven at 240 °C. Spike 10 solutions of mixed ¹⁹⁰Os –¹⁸⁵Re tracer (¹⁸⁵Re/¹⁹⁰Os = 11.2) were used in the course of this study. Osmium was purified by distillation of the volatile tetra oxide, condensed on a very small volume (2 ml) of chilled H₂SO₄, and then collected in 0.5 ml of 6.8 N HBr. The final purification of Os was accomplished by micro-distillation, following the method of Birck, Roy Barman & Capmas (1997). Os isotope ratios were determined using a SPECTROMAT ion counting-system running in peak-jumping mode. The 2σ in-run analytical uncertainties for Re and Os isotope ratios were < 0.1 % and < 0.3 %, respectively. Total procedural blanks averaged 0.1 ± 0.05 pg for Os. The isotopic composition of Os in the blank is very close to the natural composition and has a ratio of 0.112 (¹⁸⁷Os/¹⁸⁸Os). All data were blank corrected on the basis of these measurements in combination with a yield of 90 %, and an Os blank of 0.10 pg.

4. Results

4.a. Palynology

A total of 5239 miospores plus a few acritarchs were recorded from 12 productive samples (of which 4780, about 90 %, were obtained from two samples). Seventy-two species of miospores (spores and pollen grains) were identified, together with two species of megaspores (Fig. 3). Of the miospores, 63 taxa are listed in Figure 3 (the 23 most characteristic ones are illustrated in Fig. 4), the remaining ten taxa being either forms with a very wide stratigraphic range or of doubtful identity owing to low frequency and poorer state of preservation. In terms of diversity, this is comparable to the miospore assemblages described from the T–J transition interval, i.e. to those described by Lund (1977: 80 taxa identified), Pedersen & Lund (1980: 76 taxa indentified), Achilles (1981: 147 taxa identified) and the assemblages newly described from Austria (Bonis, Kürschner & Krystyn, 2009: 118 taxa identified) and from Slovakia (Ruckwied & Götz, 2009: 64 taxa identified). Of particular importance is the latest work of Bonis, Kürschner & Krystyn (2009), giving by far the most complete palynological data from the T–J transition from Austrian profiles, including the GSSP at Kuhjoch, which is taken as a reference for the current paper concerning palynology.

In the beds assigned to the Rhaetian (Fig. 3), the miospores are scarce (3–5 specimens per sample) and

Table 1. Osmium and rhenium isotopic data for selected samples (see Fig. 8)

No.	Depth in m	¹⁰⁰⁰ / ¹⁹² Os		¹⁸⁷ Os/ ¹⁸⁶ Os		¹⁸⁷ Os/ ¹⁸⁸ Os		¹⁸⁷ Re/ ¹⁸⁶ Os		¹⁸⁷ Re/ ¹⁸⁸ Os		ppt Re		ppt Os		⁸⁷ Os/ ¹⁸⁶ Os		¹⁸⁷ Os/ ¹⁸⁸ Os	
		Initial	2σ	Initial	2σ	Initial	2σ	Initial	2σ	Initial	2σ	Initial	2σ	Initial	2σ	Initial	2σ	Initial	2σ
1	703.2	35.58	0.015	5.016	0.015	0.6037	0.0018	109.67	43.3	0.6	5.22	75.7	1	73.10	0.68	4.873	0.586		
2	699.3	16.72	0.012	4.158	0.015	0.5004	0.0015	51.54	24.8	0.4	2.99	92.2	1	153.5	0.43	4.076	0.491		
3	691.0	63.52	0.014	4.781	0.017	0.5754	0.0017	195.82	256.3	3.8	30.85	251.0	3	40.79	0.38	3.932	0.473		
4	687.0	68.16	0.021	7.074	0.0026	0.8514	0.0026	210.11	796.9	12.0	95.91	726.0	7	39.33	0.37	4.434	0.534		
5	686.0	125.31	0.013	4.217	0.0015	0.5075	0.0015	386.31	114.4	1.7	13.77	56.7	1	20.50	0.19	3.838	0.462		
6	685.4	104.99	0.012	3.951	0.0014	0.4755	0.0014	323.65	122.2	1.8	14.71	72.3	1	24.37	0.23	3.546	0.427		
7	678.6	77.20	0.011	3.634	0.0013	0.4374	0.0013	237.98	220.0	3.0	26.49	177.0	2	33.00	0.30	2.905	0.350		
8	677.5	86.56	0.016	5.320	0.0019	0.6403	0.0019	266.84	446.6	6.7	53.75	320.0	3	30.18	0.28	3.841	0.462		
9	652.9	27.16	0.014	4.782	0.0017	0.5755	0.0017	83.72	83.9	1.3	10.09	192.0	2	95.41	0.89	4.504	0.542		

For depth refer to the profile in Figure 3; content of the elements in ppt (part per trillion); 2σ – error margin of measurement method; most important values discussed in the text are marked in bold.

pollen grains dominate. Just at and slightly below the sequence boundary at 678.4 m (Fig. 3), identified as the T–J boundary based on the carbon isotope curve, sequence stratigraphic correlation and occurrences of indicative megaspores of Marcinkiewicz (1971), the abundance of spores rapidly increases. In one sample at 678.6 m, just below the sequence (T–J) boundary, the frequency of miospores is 1355 specimens in one sample (many of them being grouped in tetrads), which means that the frequency of miospores just below the T–J boundary is higher by one to two orders of magnitude. In most of the Rhaetian samples the material is too sparse (3 to 5 taxa in several to 20 specimens) for reliable specification of the primary diversity of miospores. In the uppermost sample below the sequence boundary, 11 taxa were identified in 1355 specimens (93 % spores), which does not point to a high diversity. Of note also is the changing character of the palynofacies and spore/pollen grain ratio (Fig. 3) in these transitional deposits, which points to changing conditions in the interval. Prevalence of fern-derived spores may indicate a ‘fern peak’ at 678.6 m, because above the T–J boundary the frequency of spores diminishes again. However, in the uppermost sample studied (depth 642.1 m, Hettangian strata) the number of spores is even higher (3425 miospores). This sample comes from a lagoonal-marsh environment (Fig. 3). Obviously, this shift is not connected with a ‘fern peak’ associated with floral turnover, but represents a local change of environment, associated with an elevated water table in the swampy-marsh setting and the resulting character of vegetation, dominated by ferns and fern allies. Generally, the Hettangian assemblage is more diverse than the Rhaetian assemblage (only one sample with 5 taxa; other samples contain 11 to 26 taxa; Fig. 3).

Importantly, the Rhaetian miospores show lighter, dark yellow colours compared to the miospores in some samples from the Rhaetian/Hettangian transitional section, which are darker: yellow-orange, orange, and in one sample (678.6 m, just below the sequence boundary), orange-brown. Above the transitional section, miospores get lighter (dark yellow) again (Fig. 3). Generally, the miospores in a given sample show a darkening ranging by one colour step. One sample showing mostly darkened, brownish miospores shows quite a uniform darkening of the miospores. Most of the samples contain relatively light, yellow miospores, and those samples also show uniform character in colour of the miospores. Light pollen grains often show a superficial dark coating, but this was not taken into account when specifying the colours of the miospores. Spores are usually darkened uniformly; however, in pollen grains the sacs are often slightly lighter than the corps. Figure 3 shows the section 676.9–686 m with the fluctuating miospore colours. A sample at 678.6 m, just below the sequence/T–J boundary, shows the most conspicuous darkening of the miospores (orange-brown). Two other samples at 686 m and 676.8 m contain orange miospores; the rest

of the samples contain lighter, yellow-orange or dark-yellow miospores.

The uppermost Rhaetian and lowermost Jurassic transitional deposits (Fig. 3; 676.5–681 m) show a palynofloral turnover (Fig. 3): 11 taxa continue from Rhaetian to Jurassic strata, but 7 taxa disappear at the T–J boundary and 38 taxa appear above this boundary.

In the Rhaetian strata, the following miospores are characteristic: *Baculatisporites comaumensis* (Fig. 4a), *Cingulizonates rhaeticus* (Fig. 4b, c), *Deltoidospora toralis* (Fig. 4d), *Limbosporites lundblandii* (Fig. 4e, f), *Ricciisporites tuberculatus* (Fig. 4g), *Semiretisporis gothae* (Fig. 4h) (spores); and *Microreticulatisporites fuscus* (Fig. 4k), *Platysaccus niger* (Fig. 4m), *Schizosaccus keuperi* (Fig. 4o) (pollen grains). Megaspore *Trileites pinguis*, occurring in the profile studied just below the T–J boundary, is also restricted to the Rhaetian (Marcinkiewicz, 1971). Spores *Baculatisporites comaumensis*, *Cingulizonates rhaeticus*, *Deltoidospora toralis*, *Limbosporites lundblandii* and pollens *Angustisulcites klausii*, *Minutosaccus potonieii*, *Microreticulatisporites fuscus* and *Schizosaccus keuperi* show continuous occurrences in the Rhaetian interval, while the other miospores were noted in single samples.

Occurrences of *Angustisulcites klausii* (Fig. 4i), *Brachysaccus neomundanus* (Fig. 4j), *Infernopollenites gracilis*, *Microcachrydites fastidiosus*, *Minutosaccus potonieii* (Fig. 4l) and *Platysaccus nitidus* (Fig. 4n) in the Rhaetian strata in the Kamień Pomorski profile need to be commented on. They are typical of Middle Triassic (including lower Keuper in a German sense) or Carnian–Norian strata (Fijałkowska-Mader, 1999; Orłowska-Zwolińska, 1977, 1979, 1983, 1985). However, the Rhaetian age of these strata in Kamień Pomorski is proved by the presence of Rhaetian miospores (*Cingulizonates rhaeticus* and *Limbosporites lundblandii*), assigned to the Rhaetian in many works: Orłowska-Zwolińska (1979), Poland; Fisher (1972), UK; Lund (1977), Denmark and Sweden; and Achilles (1981), Germany. Therefore, presence of these ‘older’ forms can be explained either by redeposition or a longer stratigraphical range.

Just above the T–J and sequence boundary (676.6–678.4 m), the lowermost Hettangian assemblage comprises the following characteristic spores: cf. *Auritulina scanicus*, *Cingulizonates delicatus*, *Cingulizonates* cf. *inequalis*, *Concavisporites intrastriatus*, *Concavisporites umbonatus*, *Conbaculatisporites mesozoicus* (Fig. 4q), *Cyclogranisporites congestus*, *Densosporites fissus*, *Dictyophyllidites harrisi*, *Dictyophyllidites mortoni* (Fig. 4r, s), *Duplexisporites problematicus*, *Leio-triletes mesozoicus*, *Lycopodiacidites rugulatus*, *Lycopodiumsporites semimuris* (= *Retitriletes semimuris*) (Fig. 4t) and *Zebrasporites interscriptus* (Fig. 4x); and pollen grains: *Cerebropollenites thiergartii* (Fig. 4y, z), *Ovalipollis ovalis* (Fig. 4aa) and *Pinuspollenites minimus* (Fig. 4bb). The appearance of *Cerebropollenites thiergartii* is noteworthy: the FAD of this pollen grain is correlated with the beginning of the

Jurassic (FAD of *Psiloceras spelae*) in the Kuhjoch GSSP section and other profiles (Kürschner, Bonis & Krystyn, 2007; Hillebrandt *et al.* 2007; although Bonis, Kürschner & Krystyn, 2009 noted a single occurrence of *Cerebropollenites thiergartii* also *c.* 3 m below the FAD of *Psiloceras spelae*). Also, the occurrence of megaspore *Nathorstisporites hopliticus* is characteristic of the Lower Jurassic, namely, Hettangian strata (Marcinkiewicz, 1971). On the other hand, occurrences of several taxa of miospores typical of the Rhaetian (*Cingulizonates rhaeticus*, *Deltoidospora toralis*, *Limboisporites lundblandii*, *Ricciisporites tuberculatus*) continue in the lowermost Jurassic strata just above the sequence boundary at 677.5 m (Fig. 3). It is not clear to what extent these occurrences were caused by redeposition. The abundance of typically Rhaetian taxa quickly diminishes upwards, but a large-scale redeposition associated with erosion at the sequence boundary is unlikely considering the good state of preservation of these miospores. Likely, the parent plants of these miospores could still have survived into the Jurassic, albeit quickly giving way to the Jurassic flora.

Higher cored sections (635–642.1 and 649.8–653.4 m) show continuity of the assemblage noted from below, although a number of new taxa (such as *Apiculatisporites ovalis*, *Baculatisporites wellmanii*, *Cibotiumsporites jurienensis*, *Concavisporites toralis*, *Cosmosporites elegans*, *Ischyosporites variegatus*, *Lycopodiacidites rugulatus*, *Polycingulatisporites crenulatus*, *Stereisporites punctus*, *Stereisporites stereoides*, *Trachysporites asper* (Fig. 4u, v), *Trachysporites fuscus* (Fig. 4w), *Uvaesporites reissingeri*, *Zebrasporites laevigatus*, and pollen *Alisporites radialis*, cf. *Microcachrydites fastidiosus*, *Quadreculina anellaeformis*, as well as few acritarchs appear there (Fig. 3). It should be borne in mind that the cored sections between 649.8 and 653.4 m, and 637.2 and 642.4 m (Skłoby Formation) represent nearshore brackish and barrier-lagoonal/deltaic environments, respectively; thus, changes in palynofacies, frequency of miospores and the presence of acritarchs are influenced by the environmental conditions.

Collectively, miospores, associated palynofacies and macroscopic observations of floral remains and palaeosols, allow approximate reconstruction of the vegetation and its evolution through the Lower–Middle Rhaetian to the Upper Rhaetian–Early Hettangian transition in Pomerania (Fig. 3). First recorded miospores from a depth of 698–704 m in brownish mudstones with scattered carbonate nodules representing a semi-dry alluvial plain, are represented by poor miospore assemblages with pollen grains, pointing to the presence of Coniferophyta such as Pinaceae/Podocarpaceae (Barrón *et al.* 2006). Oxidized plant roots indicate the presence of palaeosols, possibly with local vegetation in wetter spots: the spores *Leiotriletes minutus*, *Baculatisporites comaumensis*, *Cingulizonates rhaeticus* and *Deltoidospora toralis* indicate the presence of Pteridophyta such as

Cyatheaceae/Dicksoniaceae (Barrón *et al.* 2006). The rare *Limboisporites lundblandii* was probably produced by Selaginellaceae (club mosses).

The following section of grey, subordinately red sandstone and mudstone (above the lower sequence boundary at 698 m and below the depth 680.9 m), was deposited in a fluvial channel/alluvial plain environment and shows similarly impoverished miospore assemblages represented mainly by pollen, with a few more taxa such as *Vitreisporites pallidus*, *Infernopollenites gracilis*, *Microreticulatisporites fuscus*, *Pinuspollenites minimus*, *Chordasporites platysaccus*, *Quadreculina* sp. and *Schizosaccus keuperi*, and the spore *Deltoidospora auritora*. Palynofacies show slightly higher abundances of structured organic matter (phytoclasts) and plant roots (palaeosols) are more frequent. The vegetation in this section implies increasing humidity upwards, with more abundant palaeosols with coalified plant roots occurring at the top, with drier periods, and the vegetation is still dominated by Pinaceae/Podocarpaceae, possibly also Caytoniales and Pteridophyta such as Cyatheaceae/Dicksoniaceae and Pinaceae/Podocarpaceae (Barrón *et al.* 2006).

The interval 677–680.9 m (with the sequence boundary at 678.4 m) is characterized by rich palynofacies, including wood, cuticle and charcoal, with very abundant miospores, accompanied also by megaspores. This is the interval of marked palynofloral turnover: a number of taxa disappear, such as the megaspore *Trileites pinguis* and characteristic spores such as *Baculatisporites comaumensis*, *Cingulizonates rhaeticus*, *Deltoidospora toralis*, *Limboisporites lundblandii* and *Semiretisporis gothae*, and pollen such as *Angustisulcites klausii*, *Minutosaccus potonieii* and *Schizosaccus keuperi*. On the other hand, spores such as *Concavisporites umbonatus*, *Conbaculatisporites mesozoicus*, *Dictyophyllidites mortoni* and *Lycopodiumsporites semimuris*, and pollen grains *Cerebropollenites thiergartii* and *Ovalipollis ovalis* appear in this interval. *Ricciisporites tuberculatus* and *Ovalipollis ovalis* appear just below the sequence boundary and continue 1.5 m above it; thus, these miospores occur exclusively within this interval. It should be noted that the disappearance of a megaspore species (i.e. *Trileites pinguis*) and spore species might reflect the disappearance of a single parent plant taxon, rather than the disappearance of two plant taxa.

Our results reveal two major palynological assemblages (Figs 3, 4, 5). The first one (678.4–703 m), with sparse miospores in its lower part (680.9–703 m) becoming much more abundant at the top (678.4–680.9 m), is typically Rhaetian and contains characteristic miospores such as *Baculatisporites comaumensis*, *Cingulizonates rhaeticus*, *Deltoidospora toralis*, *Limboisporites lundblandii*, *Semiretisporis gothae*, *Platysaccus niger* and *Schizosaccus keuperi*. A low abundance of miospores in the Lower–Middle Rhaetian section (699–703 m, below the first sequence boundary) was probably related to climatic aridity and an oxidizing environment,

Chrono-stratigraphy		Northern Calcareous Alps (Austria)				Spain		UK - Germany - Scandinavia - Poland					
		Bonis et al. 2009		Kürschner et al. 2007		Schuurman 1979	Morbey 1975	Barrón et al. 2006	Poulsen & Riding 2003 dinocysts	Orbell 1973	Lund 1977	This study	
		Hochalp.	Kuhjoch	dinocysts	terr. palyno								
JURASSIC	Hettangian	H4b	K4	<i>Dapcodinium priscum</i>	Tpi zone	Phase 5	FG Miospore Subzone	Pa3 zone	<i>Krauselisporites reissingeri</i> Zone	<i>Dapcodinium priscum</i>	Heliosporites Zone	Pinuspollenites Trachysporites Zone	Conbaculatisporites mesozoicus- Dictyophyllidites mortoni- Cerebropollenites thiergartii Zone
		H4a	K3		TH zone								
		H3											
	TRIASSIC	latest Rhaetian	X		X	Tpo zone							
Mid - Late Rhaetian	H2	K2	Rpo zone										
		H1	K1	<i>Rhaetogonyaulax rhaetica</i>	RL zone	Phase 3	Pa1 zone	<i>Rhaetipollis germanicus</i> Zone	<i>Rhaetogonyaulax rhaetica</i>	Rhaetipollis Zone	Rhaetipollis Limbosporites Zone		

Figure 5. Comparison of the biostratigraphical and palynological zonation schemes from the Northern Calcareous Alps, Spain and North-Central Europe. Based on Bonis, Kürschner & Krystyn (2009), changed and amended.

while numerous spores in the uppermost Rhaetian (678.4–680.9 m) point to a generally more humid climate. In the whole Rhaetian section (678.4–703 m) some forms show continuous occurrences (i.e. *Cingulizonates rhaeticus*, *Deltoidospora toralis*, *Limbosporites lundblandi* and *Schizosaccus keuperi*), several forms occur only within the uppermost ~ 2 m of Rhaetian strata (*Baculatisporites comaumensis*, *Cingulizonates marginatus*, *Deltoidospora crassexina*, *Ricciisporites tuberculatus*, *Semiretisporis gothae*, *Ovalipollis potovalis* and *Platysaccus niger*), and the occurrences of five other taxa are spotty.

4.b. Carbon isotopes

Carbon isotope values from palynomaceral separates ($\delta^{13}\text{C}_{\text{org}}$ = per mil deviation in $^{13}\text{C}/^{12}\text{C}$ with respect to the VPDB standard) show marked fluctuations through the succession (Fig. 6). The first conspicuous negative excursion (-29.15‰ $\delta^{13}\text{C}_{\text{org}}$ at 699.3 m) is observed in the lower part of the section (Wielichowo Beds), below the lower sequence boundary. Of note is the negative

excursion (= 'initial') with two conspicuous negative sub-peaks (-29.38‰ $\delta^{13}\text{C}_{\text{org}}$ at 691 m and -28.85‰ $\delta^{13}\text{C}_{\text{org}}$ at 686 m) separated by more positive values ($\sim -26\text{‰}$ between 686 m and 691 m), a subsequent more positive excursion (-23.67‰ $\delta^{13}\text{C}_{\text{org}}$ at 681.5 m) and a second less conspicuous negative excursion beginning at 678.6 m, followed above the upper sequence boundary at 678.4 m by a slight trend towards more positive values in the interval 676.9–677.5 m, followed by an uncored section between 676.5 and 653.4 m, for which there are no data. These trends are correlated with Hungarian, UK and Austrian isotopic profiles, after Hesselbo *et al.* (2002), Hillebrandt *et al.* (2007), Pálffy *et al.* (2007), Ruhl, Kürschner & Krystyn (2009), Ruhl, Veld & Kürschner (2010) and Korte *et al.* (2009) (Fig. 7). Two measurements obtained from the section between 649.8 and 653.4 m show less negative values. Most likely, the upper (= 'main') negative excursion occurs somewhere within the uncored section between 653.4 and 686.5 m. The uppermost section, containing both continental and brackish-marine sediment is correlated with the *Planorbis* Zone (see Pieńkowski, 2004).

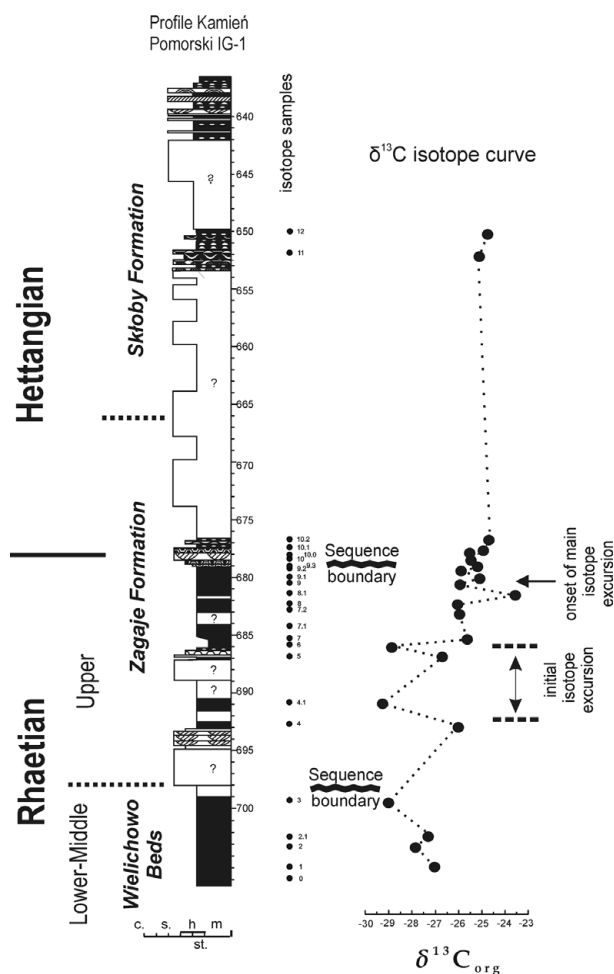


Figure 6. Carbon isotope curve with major excursions in the Kamiień Pomorski IG-1 section.

The method allowed visual observations of the residue and indicated that the palynofacies comprise mainly phytoclasts (wood, cuticle) and miospores. As the assemblages are made up of materials that originate in the terrestrial environment, the carbon isotope composition is an integrated representation of the standing vegetation, and thus also of the contemporaneous atmospheric carbon dioxide (see Hasegawa, 1997; Jahren, Arens & Harbeson, 2008). Alternatively, changes in the bulk C-isotope signature of the continental section can be explained by changes in the source of the terrestrial sedimentary organic matter, as observed among some contemporaneous terrestrial primary producers (Killops & Killops, 2005; Tyson, 1995). However, our material taken for carbon isotope analysis comes exclusively from the phytoclast (wood) fraction, which minimizes the risk of a large variation in C-isotope composition caused by heterogeneity of the organic source. Also charcoal shows no fractionation of carbon isotopes in comparison with wood (phytoclast fraction). Moreover, the surrounding palaeogeography was a rather flat, relatively uniform landscape without dramatic altitude contrasts (Pieńkowski, 2004), which precludes one of major factors of recent C-isotope fractionation, i.e.

altitude of growth of parent plants (Killops & Killops, 2005).

Whilst it is inevitable that the data obtained are far from being of a high-resolution character, at least the existence of the ‘initial’ isotope excursion (luckily, occurring in a quite expanded section of *c.* 7 m) can be proven with five samples, of which two show markedly negative values. Such values clearly indicate a major carbon isotope excursion. Considering its stratigraphical position, it is inconceivable that it could represent something other than the ‘initial’ isotope excursion.

4.c. Osmium/rhenium isotope system and iridium content

Herein we present the first suite of osmium/rhenium isotope data from the continental deposits across the T–J boundary, as well as iridium content, which can help resolve the question of a hypothetical impact and furnish evidence of igneous activity at that time. The dataset obtained from nine samples is presented in Table 1 and Figure 8. Table 1 presents both measurements of recent Re/Os isotopic contents and ratios, and the corrected, initial isotopic ratios. The calculations of initial ratios are necessary to avoid spurious isotope ratios. Firstly, the isotope ^{186}Os is unstable and contemporary results do not reflect the Early Jurassic values. Secondly, the radiogenic isotope ^{187}Os is a product of the radiogenic decay of ^{187}Re , according to the formula $^{187}\text{Re} \rightarrow ^{187}\text{Os} + e^-$. Therefore, the measurements of ^{187}Re (source of the radiogenic ^{187}Os) were used to calculate the initial (= original) content of the radiogenic ^{187}Os isotope, assuming the latest Triassic–earliest Jurassic age of the samples is *c.* 200 Ma. The higher the content of ^{187}Os is, the more radiogenic the Os-isotope ratios are. Particularly important data, such as content of non-radiogenic osmium isotope ^{192}Os and two ratios of osmium isotopes, $^{187}\text{Os}/^{186}\text{Os}$ and $^{187}\text{Os}/^{188}\text{Os}$ (marked in bold in Table 1), are presented in Figure 8. Content of ^{192}Os , the most common non-radiogenic osmium isotope, is thought to be mainly derived from igneous activity (Cohen & Coe, 2002, 2007; Kuroda *et al.* 2010). Also, a negative shift in $^{187}\text{Os}/^{188}\text{Os}$ values suggests input of non-radiogenic Os of mantle (or extraterrestrial) origin or a reduction in continentally derived Os or both (Cohen & Coe, 2002; Kuroda *et al.* 2010).

Obtained results (Table 1; Fig. 8) show that the $^{187}\text{Os}/^{188}\text{Os}$ and $^{187}\text{Os}/^{186}\text{Os}$ ratios decrease upwards in the studied section, up to the sequence boundary at 678.4 m. Particularly sharp decreases are connected with carbon isotope excursions (higher ‘subpeak’ of the ‘initial’ excursion at 686 m and a minor negative peak at 678.6 m) just below the T–J and sequence boundary. Higher up in the profile, the $^{187}\text{Os}/^{188}\text{Os}$ and $^{187}\text{Os}/^{186}\text{Os}$ ratios in Hettangian section return to positive values. The stable ^{192}Os results show a marked increase of ^{192}Os at a depth of 686 m (concomitant with the higher ‘subpeak’ of the ‘initial’ isotope excursion)

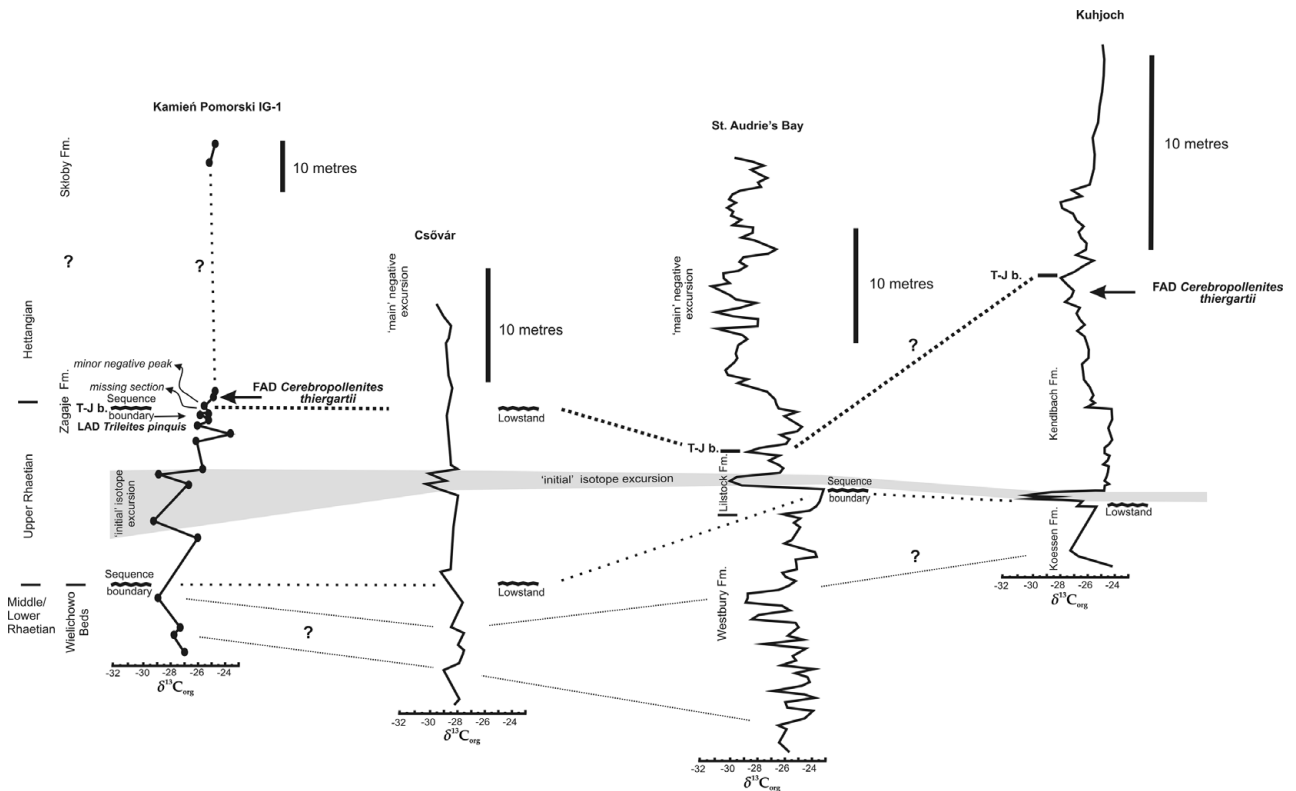


Figure 7. Correlation of $\delta^{13}\text{C}$ excursions and sequence boundaries from the Kamiień Pomorski IG-1 section with the major correlative horizons in marine Triassic–Jurassic sections. ‘Initial’ $\delta^{13}\text{C}$ excursion is shadowed; note bi-partite character of the excursion in Kamiień Pomorski, Csövár and Kuhjoch. T–J boundary is correlated with the minor subordinate negative $\delta^{13}\text{C}$ peak within the positive excursion observed in St Audrie’s Bay (Korte *et al.* 2009) and Kuhjoch in marine sections. Modified from Hesselbo *et al.* 2002; Pálffy *et al.* 2007; Kürschner, Bonis & Krystyn, 2007; Ruhl, Kürschner & Krystyn, 2009; Korte *et al.* 2009. Placement of the T–J boundary (T–J b.) based on Korte *et al.* (2009).

and a less marked increase at a depth of 677.5 m (just above the sequence boundary and inferred T–J boundary). Then, the content of ^{192}Os drops back to the Lower–Middle Rhaetian values (one sample at depth 652.1 m). The first (older) increase of the ^{192}Os content at depth 686 m coincides with a drop in $^{187}\text{Os}/^{188}\text{Os}$ ratio (Fig. 8). The upper (later) increase of ^{192}Os at 677.5 m is not coupled with a decrease in $^{187}\text{Os}/^{188}\text{Os}$ ratio. Interestingly, the disturbances in the Os isotopic system are coeval or almost coeval with two levels showing elevated polycyclic aromatic hydrocarbon (PAHs) contents (Marynowski & Simoneit, 2009, who analysed organic geochemistry in the same samples). Their first PAH positive excursion slightly pre-dates (1 m below) the major Os excursions at the depth of 686 m, the second PAH excursion coincides with the less marked excursions at the T–J boundary (677.5–678.6 m) and the third PAH disturbance at 652 m (Hettangian) is not related to any Os system disturbance (Fig. 8).

In the samples studied, all the values of the initial ratio of $^{187}\text{Os}/^{186}\text{Os}$ are around 3 or higher (Table 1; Fig. 8).

Additionally, iridium content was measured, and all the values were very low, below 10 ppt (Fig. 8).

5. Discussion

5.a. Palynology: palynofloral turnover and palaeoclimatic background

The T–J boundary is historically the least well studied of the all faunal mass extinction events and has been particularly lacking data with regard to plant palaeoecology. However, available information hints at a major palaeoecological disturbance of plant communities. Dating of the extinction event was and still is a much debated issue (e.g. Fowell & Olsen, 1993; van Veen, 1995; Olsen *et al.* 2002; Lucas & Tanner, 2007). In his seminal work, Harris (e.g. Harris, 1937) described fossil flora of the Scoresby Sund (East Greenland), and he distinguished two palynofloral assemblages: a Rhaetian *Lepidopteris* Zone and a Hettangian *Thaumatopteris* Zone. Studies of plant taxonomic ranges have revealed that up to 90 % of species became locally to regionally extinct across North America (Cornet & Olsen, 1985; Fowell & Olsen, 1993) and Greenland (Pedersen & Lund, 1980; McElwain, Beerling & Woodward, 1999; McElwain *et al.* 2007). In Greenland, considerable changes in the dominance and diversity structure of Triassic forests have been identified before the T–J boundary. Triassic communities of *Podozamites*, a

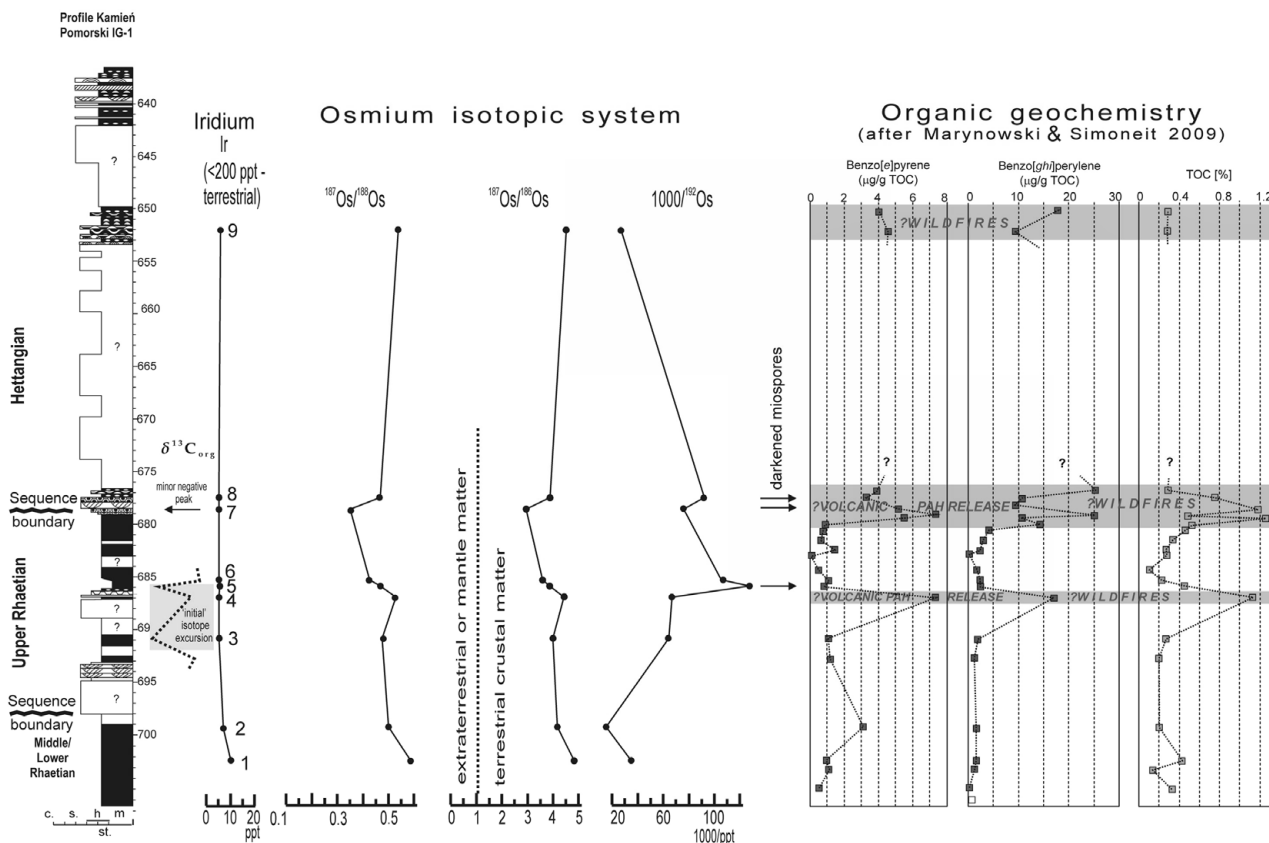


Figure 8. Changes in the iridium content and osmium isotopic system (Table 1) in the Kamień Pomorski IG-1 section (lithological column and main features of $\delta^{13}C$ on the left). Correlation with and polycyclic aromatic hydrocarbon (PAH) and TOC changes (after Marynowski & Simoneit, 2009, supplementary data) is shown. Levels with darkened miospores (see Fig. 3) are arrowed. Note two disturbance levels in the osmium isotope system concomitant with carbon isotope disturbances, PAH shifts and darkened colour of the miospores. The uppermost PAH shift is not related to carbon and Os-isotope disturbances; thus it is probably purely a wildfire effect.

broad-leaved conifer, and bennetites (*Pterophyllum* and *Anomozamites*) were replaced by lower diversity and less even (i.e. more dominant) forests, overwhelmingly dominated by taxa that had been relatively minor components of Late Triassic forests: *Czekanowskia*, *Sphenobaiera* and an osmundaceous fern (*Todites*) (McElwain *et al.* 2007; McElwain, Wagner & Hesselbo, 2009). Importantly, a climate-driven shift from a prevalence of broad-leaved taxa to a predominantly narrow-leaved assemblage contributed to increased fire activity at the T–J boundary in Greenland (Belcher *et al.* 2010a). However, estimates of diversity loss based on macrofossils are typically much higher than estimates of diversity loss based on miospores (Mander, Kürschner & McElwain, 2010). The authors explained that conflicting records of diversity loss obtained from plant macrofossils and sporomorphs are caused by the absence of reproductively specialized plants, including cycads, bennetites and the seed-fern *Lepidopteris*, from the palynofloral record. Moreover, current reports from Europe and the Tethyan domain (Kürschner & Hengreen, 2010; Cirilli, 2010) show that palynofloral composition between the Late Triassic and Hettangian was gradual and without abrupt changes and consequently claimed that the end-Triassic biotic crisis appears to have little affected palynofloral species diversity, at least in Europe. On the other hand, in North

America high-diversity pollen assemblages comprising monosulcates and monosaccates give way to lower-diversity assemblages dominated by *Classopollis*, a pollen type normally associated with hot and/or arid climate conditions, and palynofloral diversity loss is estimated at about 60% (Fowell & Olsen, 1993; Lucas & Tanner, 2007). These low-diversity pollen assemblages are confined to within 21 000 years before the T–J boundary in eastern North America as defined by a fern spike (Fowell & Olsen, 1993) and negative carbon isotope excursion. Recently, the fern spike has been correlated with the ‘initial’ carbon isotope excursion and end-Triassic extinction (Whiteside *et al.* 2010).

In Kamień Pomorski the palynofloral turnover coincides with the sequence boundary at 678.4 m. Twenty new taxa appear just above this boundary and within 2 m above it. Some typically Rhaetian spores pass into the strata immediately above the sequence boundary, but they show rapid decrease in frequency (*Cingulizonates rhaeticus* and *Limbosporites lundblandii*) and quickly disappear. Importantly, the index pollen grain *Cerebropollenites thiergartii* appears just at the sequence boundary. Several characteristic Jurassic taxa (*Concavisporites intrastratus*, *Concavisporites umbonatus*, *Conbaculatisporites mesozoicus*, *Dictyophyllidites mortoni*, *Zebrasporites interscriptus*

and *Cerebropollenites thiergartii*) show continuity throughout the rest of the Hettangian profile studied herein. *Chordasporites platysaccus*, *Pinuspollenites minimus* and *Vitreisporites pallidus* appear already in the Rhaetian strata and continue through the Jurassic section. As was previously mentioned, a hiatus at the sequence boundary could exist, which would make the transition perhaps appear more abrupt than it actually is.

The Rhaetian assemblage from Pomerania (which is referred to here as the *Cingulizonathes rhaeticus*–*Limbosporites lundblandii* association; Fig. 5) can be compared to other biostratigraphical/palynological zones in Europe, both in Tethyan and epicontinental domains (Fig. 5; Table 2; see Bonis, Kürschner & Krystyn, 2009; Lund, 1977; Pedersen & Lund, 1980; Kürschner, Bonis & Krystyn, 2007). Also in the previous works from Poland (Orłowska-Zwolińska, 1983, 1985; Marcinkiewicz & Orłowska-Zwolińska, 1994) *Limbosporites lundblandii* (along with *Cingulizonathes rhaeticus* and *Semiretisporis gothae*) are regarded as the most common and characteristic Rhaetian forms in Poland.

The narrow interval between 677 and 680.9 m (Fig. 3) could represent the transitional *Ricciisporites*–*Polypodiisporites* (Lund, 1977) or *Trachysporites*–*Porcellispora* Zone (Kürschner, Bonis & Krystyn, 2007), although in Pomerania the transitional assemblage cannot be clearly distinguished. Only *Ricciisporites tuberculatus* and *Ovalipollis ovalis* occur exclusively within this transitional zone, at the same time crossing the inferred Rhaetian–Hettangian boundary.

The Hettangian assemblage in Pomerania is referred to here as the *Conbaculatisporites mesozoicus*–*Dictyophyllidites mortoni*–*Cerebropollenites thiergartii* association (Fig. 5). All three miospore taxa characterizing Hettangian strata in Pomerania are widespread and characteristic forms, known from most of the important T–J profiles (Lund, 1977; Barrón *et al.* 2006; Kürschner, Bonis & Krystyn, 2007; Bonis, Kürschner & Krystyn, 2009 and others; Fig. 5; Table 2). *Dictyophyllidites mortoni*, *Lycopodiumsporites semimuris* and *Trachysporites fuscus* were listed by Fijałkowska (1989) as characteristic Hettangian forms from central Poland. The two cored sections, 635–642.1 m and 649.8–653.4 m, show continuity of the Jurassic palynological assemblage (eight taxa continue), although 20 new taxa are reported from these two sections. However, these new taxa do not represent any new groups of plants at a higher taxonomic level, and are still represented by Lycopodiaceae (*Uvaeisporites*, *Lycopodiacidites*, *Lycopodiumsporites*), Pteridophyta (ferns *Apiculatisporites*, *Baculatisporites*, *Cibotiumsporites*, *Concavisporites*, *Cosmosporites*, *Ischyosporites*, *Lycopodiacidites*, *Polycingulatisporites*, *Stereisporites*, *Trachysporites*, *Zebrasporites*) plus Bryophyta (rare *Stereisporites*) as chief parent plants for spores, and Coniferophyta (Pinaceae, Podocarpaceae, Caytoniales) representing

parent plants of the pollen grains (*Alisporites*, *Microcachryidites*, *Quadraeculina*, *Vitreisporites*). As mentioned above, palynofacies and miospore spectra in these two sections from Kamień Pomorski are chiefly dictated by palaeoenvironmental factors, i.e. shifting nearshore–marginal marine depositional environments. Palynofacies thus reflect flooding (transgressive)–progradation cyclicity (Fig. 3): flooding events result in relatively poorer palynomacerals with less abundant miospores and more abundant Acritarcha (interval 649.8–653.4 m), while progradational deltaic–barrier/lagoonal facies (representing delta plain–lagoon/marsh environments) show rich palynomacerals with abundant miospores, particularly spores produced by local hydrophilic plants (interval 637.2–642.4 m). Moreover, some minor fluctuations of palynofacies from lagoonal/interdistributary–delta plain environments, reflecting probable seasonal changes, have been described from the section between 637.2 and 642.4 m depth (Pieńkowski, 2004; Pieńkowski & Waksmundzka, 2009).

Comparison of T–J spores described in the present paper show a significant number of common taxa with the adjacent sedimentary basins and the Northern Tethys domain (Table 2). In contrast, there are only six taxa in common with the profiles in Asturias, Spain (of 43 listed there; Barrón *et al.* 2006) and very few (4–6) with the British profiles (Warrington & Harland, 1975; Warrington, Cope & Ivimey–Cook, 1994), but only 20 to 33 miospore taxa were identified in the British profiles at St Audrie’s and Larne. Even fewer taxa occur in common with the North American sections (Cornet & Olsen, 1985; Fowell & Olsen, 1993; Cirilli *et al.* 2009). Absence of the otherwise widespread thermophilic pollen *Corollina* sp. (*Classopollis* sp.) is notable; these pollen were noted in central Poland, some 700 km SE from Kamień Pomorski (Fijałkowska, 1992; Marcinkiewicz & Orłowska-Zwolińska, 1994; Ziaja, 2006). These pollen show very low frequencies in some other regions (i.e. East Greenland), which was attributed to palaeogeographic factors (Pedersen & Lund, 1980).

Comparison with other profiles also shows that a few stratigraphically indicative forms found in Kamień Pomorski (such as spores *Cingulizonathes rhaeticus*, *Conbaculatisporites mesozoicus*, *Limbosporites lundblandii*, *Ricciisporites tuberculatus*, *Deltoidospora toralis*, *Trachysporites fuscus* and pollen grains *Cerebropollenites thiergartii*, *Minutosaccus potonieii*, *Pinuspollenites minimus*) are more cosmopolitan than other miospores (Table 2). Collectively, these facts suggest some provinciality of the T–J palynofloral assemblages.

Perhaps, this provinciality and changing local climatic and palaeoenvironmental conditions could provide explanations for the conflicting records of T–J palynofloral turnover. Mander, Kürschner & McElwain (2010) and Kürschner & Herngreen (2010) played down the scale of this turnover, pointing to emigration and/or extirpation of taxa rather than immigration

Table 2. Occurrences of miospores from Kamień Pomorski in other regions of Europe

POLAND/THIS STUDY	North Sea Basin	East Greenland	S Germany	Austria/ Alps	Slovakia/ Tatra	Asturias/ Spain
Number of common taxa	26	19	24	21	16	6
SPORES						
<i>Acanthotriletes varius</i> Lund			*	*	*	
<i>Apiculatisporites ovalis</i> (Nilsson) Norris	*	*				
cf. <i>Auritulina scanicus</i> Nilsson						
<i>Baculatisporites comaumensis</i> (Cookson) Potonie	*	*	*			
<i>Baculatisporites wellmanii</i> (Couper) Krutzsch	*	*				
<i>Cibotiumsporites jurienensis</i> Filatoff						
<i>Cingulizonates rhaeticus</i> (Reinhardt) Schulz	*		*	*	*	
<i>Cingulizonates delicatus</i> Orłowska-Zwolińska						
<i>Cingulizonates</i> cf. <i>inequalis</i> (Madler) Lund						
<i>Cingulizonates marginatus</i> (Madler) Lund						
<i>Concavisporites intrastriatum</i> (Nilsson) Arjang			*			
<i>Concavisporites umbonatus</i> (Bolkhovitina) Schulz			*			
<i>Concavisporites toralis</i> (Leschik) Nilsson			*			
<i>Conbaculatisporites mesozoicus</i> Klaus	*	*	*		*	
<i>Cosmosporites elegans</i> (Nilsson) Achilles				*		
<i>Cyclogranisporites congestus</i> Leschik			*			
<i>Deltoidospora auritora</i> (Reinhardt) Lund	*		*		*	
<i>Deltoidospora crassexina</i> (Nilsson) Lund	*	*			*	
<i>Deltoidospora toralis</i> (Leschik) Lund	*	*		*	*	*
<i>Deltoidospora toralis</i> var. <i>media</i> Lund	*					
<i>Densosporites fissus</i> (Reinhardt) Schulz			*	*	*	
<i>Dictyophyllidites harrisi</i> Couper						
<i>Dictyophyllidites mortoni</i> (de Jersey) Playford & Dettmann			*			
<i>Duplexisporites problematicus</i> (Couper) Filatoff			*			
<i>Ischyosporites variegatus</i> (Couper) Schulz				*		*
<i>Leiotriletes minutus</i> (Knox) Potonie & Kremp			*			
<i>Limbosporites lundblandii</i> Nilsson	*	*	*	*		
<i>Lycopodiacidites rhaeticus</i> Schulz	*		*	*		
<i>Lycopodiacidites rugulatus</i> (Couper) Schulz	*	*	*	*	*	
<i>Lycopodiumsporites semimuris</i> Danze-Corsin & Laveine	*	*				
<i>Neochomotriletes triangularis</i> (Bolkhovitina) Reinhardt			*	*		
<i>Osmundacidites wellmanii</i> Couper			*			
<i>Ricciisporites tuberculatus</i> Lundblad	*	*	*	*	*	
<i>Semiretisporis gothae</i> Reinhardt				*	*	
<i>Stereisporites punctatus</i> (Klaus) Krutzsch						
<i>Stereisporites stereoides</i> Potonie & Venitz		*	*			
<i>Trachysporites asper</i> Nilsson	*	*				
<i>Trachysporites fuscus</i> Nilsson	*	*		*	*	*
<i>Tripartites mesozoicus</i> Rogalska	*					
<i>Uvaesporites reissingeri</i> (Reinhardt) Lund	*	*			*	
<i>Zebrasporites interscriptus</i> (Thiergart) Klaus	*		*	*		
<i>Zebrasporites laevigatus</i> Schulz	*		*	*		
POLLENS						
<i>Alisporites radialis</i> (Leschik) Lund	*	*		*		
<i>Angustisulcites klausii</i> Freudenthal						
<i>Brachysaccus neomundanus</i> f. <i>minor</i> (Leschik) Madler						
<i>Cerebropollenites thiergartii</i> Schulz	*	*		*		*
<i>Chordasporites platysaccus</i> Mädler						
<i>Infernopollenites gracilis</i> Pautsch						
<i>Minutosaccus potonieii</i> Mädler						
cf. <i>Microcachryidites fastidiosus</i> (Jansonius) Klaus						
<i>Microreticulatisporites fuscus</i> (Nilsson) Morbey						
<i>Ovalipollis ovalis</i> Krutzsch	*				*	
<i>Ovalipollis potovalis</i> (Potonie) Mädler						
<i>Pinuspollenites minimus</i> (Couper) Kemp		*	*	*		
<i>Platysaccus niger</i> Mädler						
<i>Platysaccus nitidus</i> Pastuch						
<i>Quadreaquilina annelaeformis</i> Maljavkina	*	*	*	*		*
<i>Quadreaquilina</i> sp.						
<i>Schizosaccus keuperii</i> Mädler					*	
<i>Taeniaesporites rhaeticus</i> Schulz	*			*		
<i>Taeniaesporites</i> sp.						
<i>Vitreisporites pallidus</i> (Reissinger) Nilsson	*	*	*	*	*	*

Note clear difference with Asturias, Spain, pointing to provincialism between North-Central Europe and the Mediterranean area.

and/or origination of taxa. According to these authors, the end-Triassic biotic crisis appears to have little affected palynofloral species diversity in Europe and Greenland. However, similarly to Fowell & Olsen

(1993), we report quite a marked palynofloral turnover at the T–J boundary. Influence of rather minor erosion and a potential missing section at the sequence boundary in Kamień Pomorski does not provide a

sufficient explanation. Perhaps, differences between T–J palynofloral assemblages could be regionally enhanced (or the opposite, masked) by changing climatic or taphonomic conditions. This issue needs further studies.

Interestingly, the palynofloral turnover, which coincides with the sequence boundary at 678.4 m, was not, at least not directly, related with crucial change in humidity of the climate: the climate was generally humid throughout deposition of the whole 677–680.9 m interval, which is proven by the presence of rich drifted floral remains, coalified plant roots and a huge amount of spores produced by Lycopodiaceae (Selaginellaceae: *Limbosporites*, *Lycopodiumsporites*) and Pteridophyta (ferns Cyatheaceae/Dicksoniaceae: *Cibotiumsporites*, *Concavisporites*; Dipteridaceae: *Conbaculatisporites*, *Deltoidospora*; Matoniaceae: *Dictyophyllidites*; Osmundaceae: *Baculatisporites*; Schizaceae: *Duplexisporites*). On the other hand, the presence of Coniferophyta (Pinaceae, Podocarpaceae) is proven by the presence of pollen grains such as *Ovalipollis potovalis*, *Quadraeculina* sp. and *Platysaccus niger* below the sequence boundary (Rhaetian section) and *Cerebropollenites thiergartii* and *Taeniasporites* sp. above this boundary (Hettangian section). If a rapid increase in humidity was not a direct factor in this marked turnover, then there must have been other environmental factors responsible for the palynofloral change in our material. Climatic changes, including a general increase in humidity, commenced above the first sequence boundary at 698 m. Judging from changes in leaf morphology and decreases in stomatal indices, McElwain, Beerling & Woodward (1999) postulated a fourfold increase in atmospheric CO₂ resulting in global warming and sudden loss of Late Triassic biodiversity, for example in East Greenland, a climate-driven shift from broad-leaved to narrow-leaved taxa and resulting fire activity at the T–J boundary (McElwain, Wagner & Hesselbo, 2009; Belcher *et al.* 2010a). Similarly, increased content of other greenhouse gases such as methane (Hesselbo *et al.* 2002) may have contributed to the climate warming. On the other hand, Hubbard & Boulter (2000) argued for a dramatic series of global temperature oscillations, including at least one colder/drier period at or just above the T–J boundary. Schoene *et al.* (2010) postulated global cooling and glaciations associated with the end-Triassic extinction period. These contradicting results suggest that the contrasts of Late Triassic climates may have been dramatic enough to trigger radical biological and ecological changes (Hubbard & Boulter, 2000; van de Schootbrugge *et al.* 2009). Indeed, dramatic release of SO₂ and sulphate aerosols (causing climate cooling), following release of CO₂ and methane (causing climate warming), with additional release of toxic pollutants such as PAHs, could have most likely been the final blow to the highly stressed end-Triassic ecosystem, as was postulated by van de Schootbrugge *et al.* (2009) and Deenen *et al.* (2010). The spore/pollen ratio in the critical boundary section between 677 and

680.9 m (Fig. 3) shows marked fluctuations expressed in palynofacies (Fig. 3), which suggest rapid climate (temperature) changes just below and at the T–J transition. Additionally, darkening of spores observed in this interval, particularly in three samples (Figs 3, 8), could have been caused by soil acidification from sulphuric acid rains during CAMP eruptions (van de Schootbrugge *et al.* 2009). On the other hand, contrasting miopore colours in one sample, named by Pieńkowski & Waksmundzka (2009) as palynofacies inversion no. 1, can be attributed to the early burial setting: miopores showing darker colours temporarily went through an early diagenetic cycle, commonly in the swamp/marshy environment, and after becoming darker they were redeposited again to be finally incorporated into the sediment. At the same time, the ‘background’ (lighter) miopores were delivered to the sediment directly from parent plants.

The presence of charcoal and the organic geochemistry indicate that despite the humid climate, forest fires occurred on the surrounding lands (Pieńkowski & Waksmundzka, 2009; Marynowski & Simoneit, 2009). A dramatic rise in fire activity has been recently attributed to the dominance of narrow-leaved plants coupled with increased lightning strikes in the much warmer climate at the beginning of the Jurassic period (Belcher *et al.* 2010a). Noteworthy is that concentrations of atmospheric oxygen reconstructed from recent experimental burn studies using the GEOCARBSULF (Belcher & McElwain, 2008) and sedimentary charcoal concentration (Glasspool & Scott, 2010) challenged the previous model estimates of a very low concentration of atmospheric O₂, ~ 12–13 %, during Late Triassic and Early Jurassic time (Berner, 2006; Algeo & Ingall, 2007). The new estimates show that the lower O₂ limit for combustion should be increased from 12 % to at least 15 % (Belcher & McElwain, 2008) or 16 % (Belcher *et al.* 2010b), and based on concentration of charcoal, O₂ atmospheric concentration was much higher, about 25 % (Glasspool & Scott, 2010). Concerning charcoal concentration, one should take notice that charcoal produced by wildfires was widely redeposited (owing to its resistance to biogenic degradation and buoyancy) and commonly shows an elevated concentration (in comparison to other palynomacerals) in high-energy environments and younger sediments. Reworking and redeposition of charcoal in high-energy environments occurred not only in alluvial environments (Marynowski & Simoneit, 2009), but also occurred in other environments, such as nearshore; therefore, fossil charcoal abundance should be taken with some caution as an ‘*in situ*’ indicator of wildfire frequency (Pieńkowski & Waksmundzka, 2009).

In addition, we would like to point out that release of toxic pollutants such as SO₂, sulphate aerosols and PAHs certainly led to defoliation, which increased forest flammability and resulting fire activity, similar to the climate-driven shift from broad-leaved to narrow-leaved taxa at the T–J boundary (McElwain, Wagner & Hesselbo, 2009; Belcher *et al.*, 2010a).

5.b. Carbon isotopes

Terrestrial organic matter displays significant inter-specific variation in isotopic composition owing to variations in the organic composition and/or pedogenic processes; thus it may be argued that only a compound-specific analysis is likely to reveal an atmospheric change in isotopic composition (Kürschner, Bonis & Krystyn, 2007; Ruhl, Kürschner & Krystyn, 2009; Ruhl, Veld & Kürschner, 2010). The obtained results reflect carbon-cycle disturbances in the atmospheric system from a limited set of plant organs. Therefore, the isotope data obtained from the palynomaceral separates (i.e. separated phytoclasts) may be the most reliable, although obtained by a very arduous method.

The carbon isotope excursions (CIEs) at the T–J boundary interval are known from many (mostly marine) successions from several continents from low to mid palaeolatitudes, and provide a robust and reproducible means of correlation. The CIE is well documented at several other former GSSP candidates including St Audrie's Bay, UK (Hesselbo *et al.* 2002), Larne, Northern Ireland (Simms & Jeram, 2006), Queen Charlotte Islands (Kunga Island and Kennecott Point combined), British Columbia (Ward *et al.* 2001, 2004; Williford *et al.* 2007), and numerous sites in Austria, including Kendelbachgraben and Tiefengraben and particularly at Kuhjoch, the GSSP for the base of the Jurassic System (Kürschner, Bonis & Krystyn, 2007; Ruhl *et al.* 2007; Hillebrandt *et al.* 2007). At most localities the CIE is divided into two excursions: the lower ('initial') and the upper ('main', although not so well characterized), separated by a positive excursion. Of note is also another negative CIE observed in older Rhaetian strata (i.e. the Westbury Fm in St Audrie's Bay, see Hesselbo *et al.* 2002). Possibly, the most marked excursion from the Westbury Fm corresponds to the oldest excursion observed in Kamień Pomorski at the depth of 699.3 m (Fig. 6). Furthermore, the position of the sequence boundaries (emergence surfaces or lowstand deposits) in St Audrie's Bay, Kuhjoch and Csövár and the most prominent sequence boundary in Kamień Pomorski at 698 m provide additional correlative constraints, separating the older Rhaetian excursions from subsequent 'initial' excursion (Fig. 6). The 'initial' excursion, was regarded as so significant, that it prompted the suggestion that isotope stratigraphy may be used to define the position of the T–J boundary (Hesselbo *et al.* 2002; Hesselbo, Robinson & Surlyk, 2004). The advantage of choosing the CIE event is that it has been widely recognized in North America and Europe. However, the isotope excursions have not so far been described from South America. The disadvantage of adopting a carbon isotope marker is that it could become unrecognizable or distorted by the occurrence of minor gaps in the succession or by post-depositional alteration; errors in identification and correlation could occur, so independent biochronological corroboration will in all cases be required. In the UK at St Audrie's Bay, the 'initial' excursion is located slightly below

the last occurrence of conodonts (top of the Cotham Member of the Lilstock Formation); in eastern North America the 'initial' excursion spans most of the prominent evolutionary events in the latest Rhaetian, such as the Newark (Passaic) palynofloral turnover and the first CAMP eruptions (Lucas & Tanner, 2007; Korte *et al.* 2009; Deenen *et al.* 2010; Whiteside *et al.* 2010). The above observations show that the 'initial' carbon isotope excursion is of great correlative significance and it coincides with the onset of magmatism in the CAMP and onset of the Late Rhaetian extinction level (Deenen *et al.* 2010; Whiteside *et al.* 2010).

In the Kamień Pomorski continental succession, this marked 'initial' negative CIE occurs at a depth of ~ 685–692 m, spanning some 7 m of sediments (Fig. 6) and is located within the range of the typical Rhaetian miospores (Fig. 4). Two negative sub-peaks of the 'initial' negative excursion, separated by a more positive value, are observed (although only in three samples). Judging from the values of $\delta^{13}\text{C}$ and its stratigraphical position, the 'bi-partite' character of the 'initial' excursion can be tentatively compared to the isotope curves obtained from many Late Rhaetian marine sections: Pálfy & Dosztály (2000), Pálfy *et al.* (2001, 2007), Götz *et al.* (2009) in Hungary; Ward *et al.* (2007) and Hesselbo, McRoberts & Pálfy (2007) in Nevada, USA; Hesselbo *et al.* (2002) in Greenland, and Ruhl, Veld & Kürschner (2010) in the Northern Calcareous Alps (even if the section including the 'initial' negative excursion is highly condensed there).

Next, the higher section between 681 and 685 m is characterized by more positive values (–26.0, –26.5 and particularly a –24.0 positive peak at 681.5 m). Above 681.5 m there is a trend back towards more negative values (–25.5, –26.0), with a slight return to more positive values at 676.9–677.5 m. The most positive peak at 681.5 m we correlate with the lower part of the positive excursion at St Audrie's Bay, separating the 'initial' and 'main' negative isotope excursions (Hesselbo *et al.* 2002).

Recently, Korte *et al.* (2009, fig. 1c) have correlated the carbon isotope curves from St Audrie's Bay and Kuhjoch, placing the T–J boundary at a secondary negative peak within the positive isotope excursion, i.e. at the top of Langport Member and Lilstock Formation (Hesselbo *et al.* 2002), although Ruhl, Kürschner & Krystyn (2009) and Deenen *et al.* (2010) still correlate the T–J boundary at Kuhjoch with the higher part of the section at St Audrie's (onset of the 'main' isotope excursion at St Audrie's or even the higher part of this profile). Based on miospores and megaspore evidence and succession of carbon isotope disturbances, we follow the correlation of Korte *et al.* (2009). Consequently, the slight trend towards more negative values above the positive excursion at 681.5 m in Kamień Pomorski (Fig. 7) is correlated with the subordinate negative peak within the positive excursion at St Audrie's, adopted also as the geochemical marker of the T–J boundary (Korte *et al.* 2009). Again, it should

be borne in mind that some section in Kamień Pomorski could be missing at the sequence boundary.

The second negative excursion is probably hidden within the uncored section between 653.5 and 676.5 m and correlation with Hettangian strata in the marine profiles of St Audrie's, New York Canyon and Tyrol is based on the appearance of *Cerebropollenites thiergartii* and a Jurassic palynomorph assemblage just above the Rhaetic palynomorph assemblage. The upper range of the 'main' isotopic excursion is unclear. In England (Hesselbo *et al.* 2002), the top of the main excursion has not been documented; in the USA and Tyrol (Ward *et al.* 2007; Hillebrandt *et al.* 2007; Kürschner *et al.* 2007; Ruhl *et al.* 2007) this excursion is terminated within the Lower Hettangian (*Psiloceras planorbis* chron), while in other profiles from Canada (Williford *et al.* 2007), this excursion extends stratigraphically higher than any other extant dataset and demonstrates that the 'main' isotope excursion does not represent a short event at all, but in fact a prolonged trend of isotopically light organic matter that extends well into the Sinemurian.

5.c. Rhenium/osmium isotopic system and iridium content

Obtained results (Table 1; Fig. 8), showing the decreasing trend of $^{187}\text{Os}/^{188}\text{Os}$ and $^{187}\text{Os}/^{186}\text{Os}$ values up to the sequence boundary at 678.4 m and increase (although not so stable) in ^{192}Os values indicates an increase in the relative supply rate of non-radiogenic Os from the mantle, most probably associated with emplacement of the CAMP. The subsequent shift towards radiogenic values in Hettangian strata reflects an increased supply of radiogenic Os owing to enhanced continental weathering (Cohen & Coe, 2002, 2007; Kuroda *et al.* 2010). A marked increase in the most common Os stable isotope (^{192}Os), coupled with a decrease in both $^{187}\text{Os}/^{188}\text{Os}$ and $^{187}\text{Os}/^{186}\text{Os}$ and $\delta^{13}\text{C}$ values ('initial' negative excursion) point to particularly intense volcanic activity at that level. $^{187}\text{Os}/^{188}\text{Os}$ and $^{187}\text{Os}/^{186}\text{Os}$ values further decrease to the top of Rhaetian strata (678.6 m), but the increase of ^{192}Os is this time slighter and occurs about 1 m higher at 677.5 m. Cohen & Coe (2002, 2007) and Kuroda *et al.* (2010) analysed the Os-isotope system in marine mudrock samples from St Audrie's Bay, UK, and pelagic deposits at Kurusu, Japan. These authors confirmed coincidence between the carbon-cycle disturbances and changes in the Os system reflecting volcanic activity versus continental weathering. Results obtained herein show that similar changes in the Os-isotope system occur also in the continental realm (fluvio-lacustrine environment) and are also linked with the carbon-cycle disturbances (particularly to the 'initial' one). In a continental environment, the herein reported decrease in the $^{187}\text{Os}/^{188}\text{Os}$ and increase in stable ^{192}Os (Fig. 8) might point to the volcanic fallout, which must have been extensive enough to reach the Pomerania area, i.e. a distance of some 1500 km (at that time) from the

CAMP (Cirilli *et al.* 2009; Muttoni *et al.* 2010; van de Schootbrugge *et al.* 2009; Deenen *et al.* 2010). Based on existing knowledge of the osmium isotopic system in the geological cycle, it is hard to point to an alternative explanation.

Moreover, van de Schootbrugge *et al.* (2009) indicated that the T–J boundary is marked by an enrichment of PAHs, which, in the absence of correlative charcoal peaks, the authors interpreted as an indication of incomplete combustion of organic matter by ascending flood basalt lava. Van de Schootbrugge *et al.* (2009) also observed that enrichment of PAHs was associated with darkening of miospores, likely caused by acid rains. The same changes (enrichment in PAHs and darkening of miospores) can be also observed in the Kamień Pomorski profile (Fig. 8). Marynowski & Simoneit (2009) performed organic geochemistry analyses in the same samples from Kamień Pomorski. According to them, three levels (one at 687 m within the 'initial' $\delta^{13}\text{C}$ excursion, a second interval 676.9–679.4 m from the T–J transitional section and a third Hettangian interval 650–653 m) show elevated PAH concentrations, with phenanthrene, fluoranthene, pyrene and benzo[ghi]perylene being most abundant fractions (Marynowski & Simoneit 2009, fig. 9 and supplementary data). Although charcoal is present throughout the Kamień Pomorski profile as dispersed, crushed and angular fragments, there are no peculiar charcoal concentrations which might be statistically correlated to the observed PAH peaks.

At the depths 686 m and 678.6 m, darkened (brown and orange-brown) miospores were observed (Figs 3, 8). Collectively, all these indicators (carbon and osmium isotopic system disturbances, darkened miospores and PAH concentrations) tend to support van de Schootbrugge *et al.* (2009), suggesting that the release of volcanic-derived pollutants such as sulphur dioxide and toxic compounds such as PAHs may have contributed to the observed $\delta^{13}\text{C}$, PAH and Os geochemical disturbances and resulting extinction. Wildfires would accomplish the whole scenario, although in our opinion PAHs were produced not only by local wildfires. Belcher *et al.* (2010a) indicated increased fire activity at the T–J boundary in Greenland due to climate-driven floral changes, which is there additionally supported by a fivefold increase in the abundance of fossil charcoal in the earliest Jurassic. Similarly, wildfires also occurred during the T–J transitional time in Poland, as documented by Marynowski & Simoneit (2009) and Pienkowski & Waksmundzka (2009).

Additionally, the Os isotopic system studied in nine samples (Table 1; Fig. 8) can also be indicative of the potential presence of extraterrestrial matter. The most common criteria applied in such studies are the detection of a positive siderophile element anomaly (enrichment of ejecta fallout matter in Os, Re, Ir and other siderophile elements at the ppb level) and the Re–Os isotopic system ($^{187}\text{Os}/^{186}\text{Os}$ as well as $^{187}\text{Os}/^{188}\text{Os}$ ratios). As the Earth's crust is characterized by a highly

radiogenic ratio of Os isotopes (high ^{187}Os content) and meteorites are characterized by the opposite (non-radiogenic ratio of Os isotopes), the Os isotopic system is regarded as the most sensitive, thus the most reliable indicator of the presence of extraterrestrial matter in sediments (Geyh & Schleicher, 1990; Dickin, 1995; Faure, 1986; Muñoz-Espadas, Martínez-Frías & Rosario, 2003). An $^{187}\text{Os}/^{186}\text{Os}$ ratio of about 1.05–1.1 (Geyh & Schleicher, 1990; Dickin, 1995) and an ^{187}Os to ^{188}Os ratio of about 0.12–0.13 (Faure, 1986; Muñoz-Espadas, Martínez-Frías & Rosario, 2003) point to the presence of extraterrestrial matter (or alternatively, also of mantle-derived material); higher values are regarded as typical of the Earth's crust. This was first shown for the Cretaceous–Palaeogene boundary by Turekian (1982), Luck & Turekian (1983) and later in other analyses (Koeberl & Shirey, 1997; Koeberl, 1998). Based on elevated iridium content at the T–J boundary in the Newark Basin, Olsen *et al.* (2002) hypothesized, that the T–J boundary supposed mass extinction was connected with an impact event and ejecta layer (recently, this view has been softened by Whiteside *et al.* 2010).

In the samples studied, all the $^{187}\text{Os}/^{186}\text{Os}$ values (initial) are between 3.838 and 4.873, and $^{187}\text{Os}/^{188}\text{Os}$ ratio (initial) ranges between 0.427 and 0.586 (Table 1; Fig. 8). These results indicate that the Os isotopic system of the levels sampled is characteristic of typical crustal rocks, namely for the sediments derived most likely from the weathered Precambrian crystalline rocks. Furthermore, Ir content is less than 5 ppt (measurement sensitivity threshold), except for one sample (depth 703.2 m) where the Ir content was 7 ppt. In conclusion, the samples studied (in respect of the $^{187}\text{Os}/^{186}\text{Os}$ and $^{187}\text{Os}/^{188}\text{Os}$ ratio values as well as the Ir content) do not contain detectable extraterrestrial (or larger amounts of mantle) matter, which lends no support to the hypothesis of a large projectile impact at the T–J boundary.

6. Conclusions

The sequence of main stages in the formation of the continental section of Kamień Pomorski IG-1 can be summarized as follows:

- (1) Early–Middle Rhaetian time was characterized by semi-dry alluvial plain sedimentation, a poor association of xeromorphic plants, red beds with carbonate pedogenesis, and at least one negative excursion on the background of less negative carbon isotope values.
- (2) A sequence boundary, probably marking the lowest sea-level (and erosion base level), followed by fluvial sedimentation coupled with a change to grey colour and the accumulation of coaly matter, indicating a change in the hydrologic cycle, a prominent ‘initial’ negative isotope excursion in organic carbon (showing a bi-partite character), concomitant marked

perturbation in the Os-isotope system (decrease in $^{187}\text{Os}/^{188}\text{Os}$ ratio, increase of stable ^{192}Os), increase in PAHs and darkening of miospores. The palynofloral association is characterized by sparse pollen grains, which lends no support for rapid warming and humidification at this level.

- (3) Positive shift in carbon isotope values.
- (4) Slight shift towards more negative carbon isotope values, second (although less marked) change in the Os isotopic system, prevalence of spores (including a ‘fern peak’ just below the T–J boundary with markedly darkened miospores), humidification of climate at the top, a second sequence boundary, frequent changes in palynofacies and inferred palaeoclimatic fluctuations, and palynofloral turnover at the sequence boundary.
- (5) Early–Middle Hettangian, brackish marine transgression in the *Planorbis* Zone, further diversification of miospores, and humid conditions.

Our analyses reveal: (1) background sediment deposition, with marked changes in the hydrologic cycle, pedogenic processes, palynofacies and colour of sediments, all pointing to gradual humidification of the climate in Late Rhaetian times, although these times were probably still punctuated by rapid and pronounced climatic fluctuations, as shown by the palynofacies and carbon isotope fluctuations; (2) the carbon isotope curve obtained from phytoclast palynomacerals, which shows significant fluctuations beginning already in the Early–Middle Rhaetian, continuing in the Late Rhaetian interval with a prominent bi-partite negative $\delta^{13}\text{C}_{\text{org}}$ excursion, correlated with the ‘initial’ excursion, and a second, much less prominent excursion, indicating the T–J boundary; (3) the composition and diversification of the latest Triassic and earliest Jurassic palynological assemblages; a total of 63 well-preserved palynomorph taxa have been recorded: 42 spore taxa, 20 pollen taxa and 1 indeterminate acritarch; two assemblages of miospores have been distinguished: the latest Triassic *Cingulizonathes rhaeticus*–*Limbosporites lundblandii* association and earliest Jurassic *Conbaculatisporites mesozoicus*–*Dictyophyllidites mortoni*–*Cerebropollenites thiergartii* association with characteristic index taxa, i.e. *C. thiergartii*, marking the beginning of the Jurassic; comparison with other European records points to some provincialism of palynoflora; (4) regional palynofloral turnover, probably reflecting a turnover of ecological dominants between Triassic and Jurassic floral communities and marked structural changes in the vegetation as reflected by potential loss of the Late Triassic xerophilous plant species; (5) after the turnover at the T–J boundary, the Jurassic recovery of new species is well marked; (6) marked fluctuation in the Os-isotope system, concomitant with the negative $\delta^{13}\text{C}_{\text{org}}$ excursions, PAH shifts (see Marynowski & Simoneit, 2009), presence of darkened miospores and floral turnover interval, which collectively point to volcanic activity (volcanic fallout) (see van de Schootbrugge *et al.* 2009); PAHs

were produced also by local wildfires (Marynowski & Simoneit, 2009; Pienkowski & Waksmundzka, 2009); (7) a lack of evidence for presence of extraterrestrial matter (osmium isotopic system, iridium content), which lends no support to the impact scenario at the T–J boundary.

Importantly, carbon and osmium isotope correlation and coeval increase in PAH content confirm that the release of pollutants such as sulphur dioxide and toxic compounds (PAHs) may have contributed to the perturbances in the climate and the crisis in the terrestrial biosphere, causing floral turnover (van de Schootbrugge *et al.* 2009). The floral turnover period commenced at the ‘initial’ carbon isotope excursion, concomitant with the onset of CAMP volcanism. Most likely, periodical atmospheric loading by CO₂, CH₄ or, on the other hand, SO₂ and sulphate aerosols and PAHs, related to eruptions of the CAMP, is inferred to have caused a series of rapid climatic reversals (including rapid temperature fluctuations, see Schoene *et al.* 2010), directly influencing the ecosystem. Thus, instead of one catastrophic event, a series of rapid climatic changes (but spanning a relatively short time and thus difficult to register) may have caused the end-Triassic disturbances in ecosystems. In our opinion, the floral turnover period in the continental realm did not end at the ‘initial’ carbon isotope excursion (Whiteside *et al.* 2010), but lasted approximately until the minor (secondary) negative excursion within the positive excursion, which is now correlated with the T–J boundary (Korte *et al.* 2009) and the intermediate unit (I.U.) of the Argana volcanic flow in Morocco (Marzoli *et al.* 2004, 2011; Deenen *et al.* 2010). Floral recovery began at the same time, but it is not clear to what extent it reflects the origination of taxa. Changes in both the carbon and osmium isotopic systems, coupled with PAH content, suggest that the biotic changes in the continental environment were compatible with a global crisis triggered by the near synchronous (Marzoli *et al.* 2011) end-Triassic volcanism and implies that the continental ecosystem and marine ecosystem were affected more or less simultaneously (Cirilli *et al.* 2009; Muttoni *et al.* 2010; Korte *et al.* 2009; van de Schootbrugge *et al.* 2009; Deenen *et al.* 2010; Schoene *et al.* 2010; Kuroda *et al.* 2010). Their and our data demonstrate that the carbon and osmium isotope disturbances at the T–J transition were characteristic not just of surface seawater, in which it might be argued the isotope signal only represents localized oceanographic processes, but also the contemporaneous atmosphere and terrestrial biosphere, where localized anomalies matching those in the ocean are inconceivable. Jurassic floral renewal is related to climate stabilization. Thus, we propose here various key abiotic environmental changes that increased extirpation or extinction risk just before and at the T–J boundary. Our palaeoecological analysis reveals a significant replacement of the dominant Triassic palynotaxa with new dominants in Jurassic communities. It is not clear how widespread the

palynofloral turnover observed in Pomerania was and to what extent it was dictated by the local ecological or taphonomical conditions. Other data, pointing to gradual palynofloral changes across the T–J boundary (Mander, Kürschner & McElwain, 2010; Cirilli, 2010; Kürschner & Herengreen, 2010) open up the question of whether the observed palynofloral turnover here was more or less localized. Provincialism and local palaeoenvironmental/taphonomical conditions could have played a more significant role in observed palynofloral changes at the T–J boundary. If the palaeoecological changes described from the Pomeranian borehole are a basin-wide phenomenon, they are likely to have contributed significantly to T–J faunal change by altering the dominant forms of terrestrial primary productivity.

Acknowledgements. This work was financed by the Polish scientific funds as the project N307 011 31/0941 – our thanks go to Prof. Grzegorz Racki of Silesia University, Poland, for his support in acceptance of this grant. We thank Prof. Stephen Hesselbo of Oxford University, UK, and Dr Josef Pálfy from the Research Group for Palaeontology, Hungarian Academy of Sciences–Hungarian Natural History Museum, for all valuable suggestions and comments. We are grateful to Prof. Paul Olsen of Columbia University (USA) and to an anonymous reviewer for discerning reviews, which improved the paper. Prof. Michael Joachimski, Head of the Stable Isotope Laboratory, GeoZentrum Nordbayern, Germany, performed carbon isotope analyses. Prof. Zdzisław Bełka of Poznań University, Poland, carried out osmium and rhenium isotope analyses. This is a contribution to IGCP project 506 ‘Marine and Non-marine Jurassic: Global Correlation and Major Geological Events’.

References

- ACHILLES, H. 1981. Die rhaetische und liassische Mikroflora Frankens. *Palaeontographica Abteilung B Paläophytologie* **179**, 1–86.
- ALGEO, T. J. & INGALL, E. 2007. Sedimentary C_{org}:P ratios, paleocean ventilation, and Phanerozoic atmospheric pO₂. *Palaeogeography, Palaeoclimatology, Palaeoecology* **256**, 130–55.
- BARRÓN, E., GÓMEZ, J. J., GOY, A. & PIEREN, A. P. 2006. The Triassic–Jurassic boundary in Asturias (northern Spain): palynological characterisation and facies. *Review of Palaeobotany and Palynology* **138**, 187–208.
- BEERLING, D. & BERNER, R. 2002. Biogeochemical constraints on the Triassic–Jurassic boundary carbon cycle event. *Global Biogeochemical Cycles* **16**, 1–13.
- BELCHER, C. M., MANDER, L., REIN, G., JERVIS, F. X., HAWORTH, M., HESSELBO, S. P., GLASSPOOL, I. J. & MCELWAIN, J. C. 2010a. Increased fire activity at the Triassic/Jurassic boundary in Greenland due to climate-driven floral change. *Nature Geoscience* **3**, 426–9.
- BELCHER, C. M. & MCELWAIN, J. C. 2008. Limits for combustion in low O₂ redefine paleoatmospheric predictions for the Mesozoic. *Science* **321**, 1197–200.
- BELCHER, C. M., YEARSLEY, J. M., HADDEN, R. M., MCELWAIN, J. C. & REIN, G. 2010b. Baseline intrinsic flammability of Earth’s ecosystem estimated from paleoatmospheric oxygen over the past 350 million years. *Proceedings of the National Academy of Sciences* **107**, 22448–53.

- BERNER, R. A. 2006. GEOCARBSULF: a combined model for Phanerozoic atmospheric O₂ and CO₂. *Geochimica et Cosmochimica Acta* **70**, 5653–64.
- BIRCK, J. L., ROY BARMAN, M. & CAPMAS, F. 1997. Re–Os isotopic measurements at the femtomole level in nature samples. *Geostandards Newsletter* **20**, 19–27.
- BONIS, N. R., KÜRSCHNER, W. M. & KRYSSTYN, L. 2009. A detailed palynological study of the Triassic–Jurassic transition in key sections of the Eiberg Basin (Northern Calcareous Alps, Austria). *Review of Palaeobotany and Palynology* **156**, 376–400.
- BRAUNS, C. M. 2001. A rapid, low-blank technique for the extraction of osmium from geological samples. *Chemical Geology* **176**, 379–84.
- CIRILLI, S. 2010. Upper Triassic–lowermost Jurassic palynology and palynostratigraphy: a review. In *The Triassic Timescale* (ed. S. G. Lucas), pp. 285–314. Geological Society of London, Special Publication no. 334.
- CIRILLI, S., MARZOLI, A., TANNER, L., BERTRAND, H., BURATTI, N., JOURDAN, F., BELLINI, G., KONTAK, D. & RENNE, P. R. 2009. Latest Triassic onset of the Central Atlantic Magmatic Province (CAMP) volcanism in the Fundy Basin (Nova Scotia): new stratigraphic constraints. *Earth and Planetary Science Letters* **286**, 514–25.
- COHEN, A. S. & COE, A. L. 2002. New geochemical evidence for the onset of volcanism in the Central Atlantic magmatic province and environmental change at the Triassic–Jurassic boundary. *Geology* **30**, 267–70.
- COHEN, A. S. & COE, A. L. 2007. The impact of the Central Atlantic Magmatic province on climate and on the Sr and Os-isotope evolution of sea water. *Palaeogeography, Palaeoclimatology, Palaeoecology* **244**, 374–90.
- CORNET, B. & OLSEN, P. E. 1985. A summary of the biostratigraphy of the Newark Supergroup of eastern North America with comments on provinciality. In *Congreso Latinoamericano de Paleontología Mexico, Simposio Sobre Floras del Triásico Tardío, su Fitogeografía y Paleología, Memoria* (ed. R. Weber III), pp. 67–81. Mexico City: UNAM Instituto de Geología.
- DADLEZ, R. 1969. Stratigraphy of the Lias in Western Poland. *Prace Instytutu Geologicznego* **57**, 1–92 (in Polish, English summary).
- DADLEZ, R. 1972. Kamień Pomorski IG-1. *Profile Głębokich Otworów Wiertniczych Instytutu Geologicznego* **1**, 1–150 (in Polish, English summary).
- DADLEZ, R., IWANOW, A., LESZCZYŃSKI, K. & MAREK, S. 1998. Tectonic Map of the Zechstein-Mesozoic Complex in the Polish Lowlands 1: 500,000. Polish Geological Institute.
- DEENEN, M. H. L., RUHL, M., BONIS, N. R., KRIJGSMAN, W., KÜRSCHNER, W. M., REITSMA, M. & VAN BERGEN, M. J. 2010. A new chronology for the end-Triassic mass extinction. *Earth and Planetary Science Letters* **291**, 113–25.
- DICKIN, A. P. 1995. The Re–Os system. In *Radiogenic Isotope Geology* (ed. A. P. Dickin), pp. 202–24. Cambridge: Cambridge University Press.
- FAURE, G. 1986. *Principles of Isotope Geology*, 2nd ed. New York: J. Wiley and Sons, 589 pp.
- FIJAŁKOWSKA, A. 1989. Badania sporowo-pyłkowe osadów dolnego liasu w profilu Skarżysko-Kamienna IG 1. *Kwartalnik Geologiczny* **33**, 199–208 (in Polish, English summary).
- FIJAŁKOWSKA, A. 1992. Palynostratigraphy of the Keuper and Rhaetic in north-western margin of the Holy Cross Mts. *Geological Quarterly* **36**, 199–220.
- FIJAŁKOWSKA-MADER, A. 1999. Palynostratigraphy, palaeoecology and palaeoclimatology of the Triassic in South-eastern Poland. In *Epicontinental Triassic*, Vol. 1 (eds G. H. Bachmann & I. Lerche), pp. 601–27. *Zentralblatt für Geologie und Paläontologie*, Part I (1998)/7–8.
- FISHER, M. J. 1972. The Triassic palynofloral succession in England. *Geoscience and Man* **4**, 101–9.
- FOWELL, S. J. & OLSEN, P. E. 1993. Time calibration of Triassic–Jurassic microfossil turnover, eastern North America. *Tectonophysics* **222**, 361–9.
- GALLI, M. T., JADOUL, F., BERNASCONI, S. M. & WEISSERT, H. 2005. Anomalies in global carbon cycling and extinction at the Triassic/Jurassic boundary: evidence from a marine C-isotope record. *Palaeogeography, Palaeoclimatology, Palaeoecology* **216**, 203–14.
- GEYH, M. A. & SCHLEICHER, H. 1990. Rhenium/osmium (¹⁸⁷Re/¹⁸⁷Os) method. In *Absolute Age Determination* (eds M. A. Geyh & H. Schleicher), pp. 111–14. Berlin, Heidelberg: Springer-Verlag.
- GLASSPOOL, I. J. & SCOTT, C. 2010. Phanerozoic concentrations of atmospheric oxygen reconstructed from sedimentary charcoal. *Nature Geoscience* **3**, 627–30.
- GÖTZ, A. E., RUCKWIED, K., PÁLFY, J. & HAAS, J. 2009. Palynological evidence of synchronous changes within the terrestrial and marine realm at the Triassic/Jurassic boundary (Csövár section, Hungary). *Review of Palaeobotany and Palynology* **156**, 401–9.
- GUÉX, J., BARTOLINI, A., ATUDOREI, V. & TAYLOR, D. 2004. High-resolution ammonite and carbon isotope stratigraphy across the Triassic–Jurassic boundary at New York Canyon (Nevada). *Earth and Planetary Science Letters* **225**, 29–41.
- HAAS, J. & TARDY-FILACZ, E. 2004. Facies changes in the Triassic–Jurassic boundary interval in an intraplateau basin succession at Csovar (Transdanubian Range, Hungary). *Sedimentary Geology* **168**, 19–48.
- HALLAM, A. 1997. Estimates of the amount and rate of sea-level change across the Rhaetic–Hettangian and Pliensbachian–Toarcian boundaries (latest Triassic to Early Jurassic). *Journal of the Geological Society, London* **154**, 773–9.
- HALLAM, A. 2002. How catastrophic was the end-Triassic mass extinction? *Lethaia* **35**, 147–57.
- HALLAM, A. & WIGNALL, P. B. 1997. *Mass Extinctions and Their Aftermath*. Oxford: Oxford University Press, 320 pp.
- HALLAM, A. & WIGNALL, P. B. 1999. Mass extinctions and sea-level changes. *Earth-Science Reviews* **48**, 217–50.
- HARRIS, T. M. 1937. The fossil flora of Scoresby Sound East Greenland. 5. Stratigraphic relations. *Meddelelser om Grønland* **112**, 1–114.
- HASEGAWA, T. 1997. Cenomanian–Turonian carbon isotope events recorded in terrestrial organic matter from northern Japan. *Palaeogeography, Palaeoclimatology, Palaeoecology* **130**, 251–73.
- HESELBO, S. P., MCROBERTS, C. A. & PÁLFY, J. 2007. Triassic/Jurassic boundary events: problems, progress, possibilities. *Palaeogeography, Palaeoclimatology, Palaeoecology* **244**, 1–10.
- HESELBO, S. P., ROBINSON, S. A. & SURLYK, F. 2004. Sea-level change and facies development across potential Triassic–Jurassic boundary horizons, SW Britain. *Journal of the Geological Society, London* **161**, 365–79.
- HESELBO, S. P., ROBINSON, S. A., SURLYK, F. & PIASECKI, S. 2002. Terrestrial and marine extinction at the

- Triassic–Jurassic boundary synchronized with major carbon-cycle perturbation: a link to initiation of massive volcanism? *Geology* **30**, 251–4.
- HILLEBRANDT, A. V., KRYSZYN, I. & KÜRSCHNER, W. M., with contributions by BOWN, P., MCROBERTS, M., UHL, M., SIMMS, M., TOMASOVYCH, A. & ULRICHS, M. 2007. A candidate GSSP for the base of the Jurassic in the Northern Calcareous Alps (Kuhjoch section; Karwendel Mountains, Tyrol, Austria). *International Subcommission on Jurassic Stratigraphy Newsletter* **34**, 1–38.
- HOUNSLOW, M. W., POSEN, P. E. & WARRINGTON, G. 2004. Magnetostratigraphy and biostratigraphy of the Upper Triassic and lowermost Jurassic succession, St. Audrie's Bay, UK. *Palaeogeography, Palaeoclimatology, Palaeoecology* **213**, 331–58.
- HUBBARD, R. N. L. B. & BOULTER, M. C. 2000. Phytogeography and paleoecology in Western Europe and Eastern Greenland near the Triassic–Jurassic boundary. *Palaios* **15**, 120–31.
- JAHREN, A. H., ARENS, N. C. & HARBESON, S. A. 2008. Prediction of atmospheric $\delta^{13}\text{C}_{\text{CO}_2}$ using fossil plant tissues. *Reviews of Geophysics* **46**, RG1002, doi:10.1029/2006RG000219.
- KILLOPS, S. & KILLOPS, V. 2005. *Introduction to Organic Geochemistry*. Oxford: Blackwell Publishing.
- KOEBERL, C. 1998. Identification of meteoritic components in impactites. In *Meteorites: Flux with Time and Impact Effects* (eds M. M. Grady, R. Hutchison, G. J. H. McCall & D. A. Rothery), pp. 133–53. Geological Society of London, Special Publication no. 140.
- KOEBERL, C. & SHIREY, S. B. 1997. Re–Os isotope systematics as a diagnostic tool for the study of impact craters and distal ejecta. *Palaeogeography, Palaeoclimatology, Palaeoecology* **132**, 25–46.
- KORTE, C., HESSELBO, S. P., JENKYN, H. C., RICKABY, R. E. M. & SPÖTL, C. 2009. Palaeoenvironmental significance of carbon- and oxygen-isotope stratigraphy of marine Triassic–Jurassic boundary sections in SW Britain. *Journal of the Geological Society, London* **166**, 431–45.
- KÜRSCHNER, W. M., BONIS, N. R. & KRYSZYN, I. 2007. Carbon-isotope stratigraphy of the Triassic–Jurassic transition in the Tiefengraben section, Northern Calcareous Alps. *Palaeogeography, Palaeoclimatology, Palaeoecology* **244**, 257–80.
- KÜRSCHNER, W. M. & HERNGREEN, W. 2010. Triassic palynology of central and northwestern Europe: a review of palynofloral diversity patterns and biostratigraphic subdivisions. In *The Triassic Timescale* (ed. S. G. Lucas), pp. 263–83. Geological Society of London, Special Publication no. 334.
- KUMP, L. R. & ARTHUR, M. A. 1999. Interpreting carbon-isotope excursions: carbonates and organic matter. *Chemical Geology* **161**, 181–98.
- KURODA, J., HORI, R. S., SUZUKI, K., GRÖCKE, D. R. & OHKOUCHI, N. 2010. Marine osmium isotope record across the Triassic–Jurassic boundary from a Pacific pelagic site. *Geology* **38**, 1095–8.
- LINDSTRÖM, S. & ERLSTRÖM, M. 2006. The Late Rhaetian transgression in southern Sweden: regional (and global) recognition and relation to the Triassic–Jurassic boundary. *Palaeogeography, Palaeoclimatology, Palaeoecology* **241**, 339–72.
- LUCAS, S. G. & TANNER, L. H. 2007. The nonmarine Triassic–Jurassic boundary in the Newark Supergroup of eastern North America. *Earth-Science Reviews* **84**, 1–20.
- LUCK, J. M. & TUREKIAN, K. K. 1983. Osmium 187/Osmium 186 in manganese nodules and the Cretaceous–Tertiary boundary. *Science* **222**, 613–15.
- LUND, J. 1977. Rhaetic to Lower Liassic palynology of the onshore south-eastern North Sea Basin. *Danmarks Geologiske Undersøgelse II* **109**, 1–81.
- MANDER, L., KÜRSCHNER, W. M. & MCELWAIN, C. 2010. An explanation for conflicting records of Triassic–Jurassic plant diversity. *Proceedings of the National Academy of Sciences* **107**, 15351–6.
- MARCINKIEWICZ, T. 1971. The stratigraphy of the Rhaetian and Lias in Poland based on megaspore investigations. *Prace Instytutu Geologicznego* **65**, 1–58 (in Polish, English summary).
- MARCINKIEWICZ, T. & ORŁOWSKA-ZWOLIŃSKA, T. 1994. Miospores, megaspores and *Lepidopteris ottonis* (Goepfert) Schimper in the uppermost Triassic deposits from Poland. *Geological Quarterly* **38**, 97–116.
- MARYNOWSKI, L. & SIMONEIT, B. R. T. 2009. Wide-spread Late Triassic to Early Jurassic wildfire records from Poland: evidence from charcoal and pyrolytic polycyclic aromatic hydrocarbons. *Palaios* **24**, 785–98.
- MARZOLI, A., BERTRAND, H., KNIGHT, K. B., CIRILLI, S., BURATTI, N., VERATI, C., NOMADE, S., RENNE, P. R., YUBI, N., MARTINI, R., ALLENBACH, K., NEUWERTH, R., RAPAILLE, C., ZANINETTI, L. & BELLINI, G. 2004. Synchrony of the Central Atlantic Magmatic Province and the Triassic–Jurassic boundary climatic and biotic crisis. *Geology* **32**, 973–6.
- MARZOLI, A., JOURDAN, F., PUFFER, J. H., CUPPONE, T., TANNER, L. H., WEEMS, R. E., BERTRAND, H., CIRILLI, S., BELLINI, G. & DE MIN, A. 2011. Timing and duration of the Central Atlantic magmatic province in the Newark and Culpeper basins, eastern U.S.A. *Lithos* **122**, 175–88.
- MCELWAIN, J. C., BEERLING, D. J. & WOODWARD, F. I. 1999. Fossil plants and global warming at the Triassic–Jurassic boundary. *Science* **285**, 1386–90.
- MCELWAIN, J. C., POPA, M. E., HESSELBO, S. P., HAWORTH, M. & SURLYK, F. 2007. Macroecological responses of terrestrial vegetation to climatic and atmospheric change across the Triassic/Jurassic boundary in East Greenland. *Paleobiology* **33**, 547–73.
- MCELWAIN, J. C., WAGNER, P. & HESSELBO, S. P. 2009. Fossil plant relative abundances indicate sudden loss of late Triassic biodiversity in East Greenland. *Science* **324**, 1554–6.
- MCROBERTS, C. A. & NEWTON, C. R. 1995. Selective extinction among end-Triassic European bivalves. *Geology* **23**, 102–4.
- MORBAY, S. J. 1975. The palynostratigraphy of the Rhaetian stage, Upper Triassic in the Kendlbachgraben, Austria. *Palaeontographica Abteilung B Paläophytologie* **152**, 1–75.
- MORTON, N. 2008a. Selection and voting procedures for the base Hettangian. *International Subcommission on Jurassic Stratigraphy Newsletter* **35**, 67.
- MORTON, N. 2008b. Details of voting on proposed GSSP and ASSP for the base of the Hettangian Stage and Jurassic System. *International Subcommission on Jurassic Stratigraphy Newsletter* **35**, 74.
- MORTON, N., WARRINGTON, G. & BLOOS, G. 2008. Foreword. *International Subcommission on Jurassic Stratigraphy Newsletter* **35**, 68–73.
- MUÑOZ-ESPADAS, M. J., MARTINEZ-FRIAS, J. & ROSARIO, L. 2003. Main geochemical signatures related to meteoritic impacts in terrestrial rocks: a review. In *Impact Markers*

- in the *Stratigraphic Record* (eds C. Koeberl & M. J. Muñoz-Espadas), pp. 65–90. Berlin: Springer.
- MUTTONI, G., KENT, D. V., JADOUL, F., OLSEN, P. E., RIGO, M., GALLI, M. T. & NICORA, A. 2010. Rhaetian magneto-biostratigraphy from the Southern Alps (Italy): constraints on Triassic chronology. *Palaeogeography, Palaeoclimatology, Palaeoecology* **285**, 1–16.
- OLSEN, P. E., KENT, D. V., SUES, H. D., KOEBERL, C., HUBER, H., MONTANARI, A., RAINFORTH, E. C., FOWELL, S. J., SZAJNA, M. J. & HARTLINE, B. W. 2002. Ascent of dinosaurs linked to an iridium anomaly at the Triassic–Jurassic boundary. *Science* **296**, 1305–7.
- ORBELL, G. 1973. Palynology of the British Rhaeto–Liassic. *Bulletin of Geological Survey of Great Britain* **44**, 1–44.
- ORŁOWSKA-ZWOLIŃSKA, T. 1977. Palynological correlation of the Bunter and Muschelkalk in selected profiles from Western Poland. *Acta Geologica Polonica* **27**, 417–30.
- ORŁOWSKA-ZWOLIŃSKA, T. 1979. Miospory. In *Budowa geologiczna Polski. 3. Atlas skamieniałości przewodnich i charakterystycznych. 2a. Mesozoik-Trias* (ed. L. Malinowska), pp. 159–291. Warsaw: Wydawnictwa Geologiczne (in Polish, English summary).
- ORŁOWSKA-ZWOLIŃSKA, T. 1983. Palynostratigraphy of the upper part of Triassic epicontinental sediments in Poland. *Prace Instytutu Geologicznego* **104**, 1–88.
- ORŁOWSKA-ZWOLIŃSKA, T. 1985. Palynological zones of the Polish epicontinental Triassic. *Bulletin Polish Academy of Sciences, Earth Sciences* **33**, 107–17.
- PÁLFY, J. 2003. Volcanism of the Central Atlantic Magmatic Province as a potential driving force in the end-Triassic mass extinction. In *The Central Atlantic Magmatic Province: Insights from fragments of Pangea* (eds W. E. Hames, J. G. McHone, P. Renne & C. Ruppel), pp. 255–67. American Geophysical Union, Geophysical Monograph vol. 136. Washington, DC, USA.
- PÁLFY, J. & DOSZTALY, L. 2000. A new marine Triassic–Jurassic boundary section in Hungary. *GeoResearch Forum* **6**, 173–80.
- PÁLFY, J., SMITH, P. L. & MORTENSEN, J. K. 2000. A U–Pb and $^{40}\text{Ar}/^{39}\text{Ar}$ time scale for the Jurassic. *Canadian Journal of Earth Sciences* **37**, 923–44.
- PÁLFY, J., DEMENY, A., HAAS, J., HETENYI, M., ORCHARD, M. J. & VETO, I. 2001. Carbon isotope anomaly and other geochemical changes at the Triassic–Jurassic boundary from a marine section in Hungary. *Geology* **29**, 1047–50.
- PÁLFY, J., DEMENY, A., HAAS, J., CARTER, E. S., GOROG, A., HALASZ, D., ORAVECZ-SCHIEFFER, A., HETENYI, M., MARTON, E., ORCHARD, M. J., OZSVART, P., VETI, I. & ZAJZON, N. 2007. Triassic–Jurassic boundary events inferred from integrated stratigraphy of the Csővár section, Hungary. *Palaeogeography, Palaeoclimatology, Palaeoecology* **244**, 11–33.
- POULSEN, N. E. & RIDING, J. B. 2003. The Jurassic dinoflagellate cyst zonation of subboreal Northwest Europe. *Geological Survey of Denmark and Greenland Bulletin* **1**, 115–44.
- PEDERSEN, K. R. & LUND, J. J. 1980. Palynology of the plant-bearing Rhaetian to Hettangian Kap Stewart Formation, Scoresby Sund, East Greenland. *Review of Palaeobotany and Palynology* **31**, 1–69.
- PIEŃKOWSKI, G. 2004. The epicontinental Lower Jurassic of Poland. *Polish Geological Institute Special Papers* **12**, 1–154.
- PIEŃKOWSKI, G. & WAKSMUNDZKA, M. 2009. Palynofacies in Lower Jurassic epicontinental deposits of Poland: tool to interpret sedimentary environments. *Episodes* **32**, 21–32.
- RUCKWIED, K. & GÖTZ, A. E. 2009. Climate change at the Triassic/Jurassic boundary: palynological evidence from the Furkaska section (Tatra Mountains, Slovakia). *Geologica Carpathica* **60**, 139–49.
- RUHL, M., KÜRSCHNER, W. M. & KRYSSTYN, L. 2009. Triassic–Jurassic organic carbon isotope stratigraphy of key sections in the western Tethys realm (Austria). *Earth and Planetary Science Letters* **281**, 169–87.
- RUHL, M., KÜRSCHNER, W. M., REICHAERT, G. J. & KRYSSTYN, L. 2007. Detailed carbon isotope analyses of Triassic–Jurassic key sections in the western Tethyan realm. *New Mexico Museum of Natural History and Sciences Bulletin* **41**, 368.
- RUHL, M., VELD, H. & KÜRSCHNER, W. M. 2010. Sedimentary organic matter characterization of the Triassic–Jurassic boundary GSSP at Kuhjoch (Austria). *Earth and Planetary Science Letters* **292**, 17–26.
- SEPHTON, M. A., AMOR, K., FRANCHI, I. A., WIGNALL, P. B., NEWTON, R. & ZONNEVELD, J.-P. 2002. Carbon and nitrogen isotope disturbances and an end-Norian (Late Triassic) extinction event. *Geology* **30**, 1119–22.
- SIMMS, M. J. 2007. Uniquely extensive soft-sediment deformation in the Rhaetian of the UK: evidence for earthquake or impact? *Palaeogeography, Palaeoclimatology, Palaeoecology* **244**, 407–23.
- SIMMS, M. J. & JERAM, A. J. 2006. Waterloo Bay, Larne, Northern Ireland: a potential GSSP for the base of the Jurassic System. *Volumina Jurassica* **4**, 297–8.
- SCHOENE, B., GUEX, J., BARTOLINI, A., SCHALTEGGER, U. & BLACKBURN, T. 2010. Correlating the end-Triassic mass extinction and flood basalt volcanism at the 100 ka level. *Geology* **38**, 387–90.
- SCHUURMAN, W. M. L. 1979. Aspects of late Triassic palynology. 3. Palynology of latest Triassic and earliest Jurassic deposits of the northern limestone alps in Austria and southern Germany, with special reference to a palynological characterization of the Rhaetian stage in Europe. *Review of Palaeobotany and Palynology* **27**, 53–75.
- TANNER, L. H., LUCAS, S. G. & CHAPMAN, M. G. 2004. Assessing the record and causes of Late Triassic extinctions. *Earth-Science Reviews* **65**, 103–39.
- TUREKIAN, K. K. 1982. Potential of $^{187}\text{Os}/^{186}\text{Os}$ as a cosmic versus terrestrial indicator in high iridium layers of sedimentary strata. *Geological Society of America Special Paper* **190**, 243–9.
- TYSON, R. V. 1995. *Sedimentary Organic Matter: Organic Facies and Palynofacies*. London: Chapman & Hall.
- VAN DE SCHOOTBRUGGE, B., QUAN, T. M., LINDSTRÖM, S., PÜTTMANN, W., HEUNISCH, C., PROSS, J., FIEBIG, J., PETSCHICK, R., RÖHLING, H.-G., RICHOS, S., ROSENTHAL, Y. & FALKOWSKI, P. G. 2009. Floral changes across the Triassic/Jurassic boundary linked to flood basalt volcanism. *Nature Geoscience* **2**, 589–94.
- VAN VEEN, P. M. 1995. Time calibration of Triassic/Jurassic microfossil turnover, eastern North America – Comment. *Tectonophysics* **245**, 93–5.
- WARD, P. D., HAGGART, J. W., CARTER, E. S., WILBUR, D., TIPPER, H. W. & EVANS, T. 2001. Sudden productivity collapse associated with the Triassic–Jurassic boundary mass extinction. *Science* **292**, 1148–51.
- WARD, P. D., GARRISON, G. H., HAGGART, J. W., KRING, D. A. & BEATTIE, M. J. 2004. Isotopic evidence bearing on Late Triassic extinction events, Queen Charlotte Islands, British Columbia, and implications for the duration and the cause of the Triassic/Jurassic mass extinction. *Earth and Planetary Science Letters* **224**, 589–600.

- WARD, P. D., GARRISON, G. H., WILLIFORD, K. H., KRING, D. A., GOODWIN, D., BEATTIE, M. & MCROBERTS, C. A. 2007. The organic carbon isotopic and paleontological record across the Triassic-Jurassic boundary at the candidate GSSP section at Ferguson Hill, Muller Canyon, Nevada, USA. *Palaeogeography, Palaeoclimatology, Palaeoecology* **244**, 281–90.
- WARRINGTON, G. & HARLAND, R. 1975. Palynology of the Trias and Lower Lias of the Larne Borehole. *Bulletin of the Geological Survey of Great Britain* **50**, 37–50.
- WARRINGTON, G., COPE, J. C. W. & IVIMEY-COOK, H. C. 1994. St. Audrie's Bay, Somerset, England: a candidate Global Stratotype Section and Point for the base of the Jurassic System. *Geological Magazine* **133**, 191–200.
- WHITESIDE, J. H., OLSEN, P. E., EGLINTON, T., BROOKFIELD, M. E. & SAMBROTTO, R. N. 2010. Compound-specific carbon isotopes from Earth's largest flood basalt eruptions directly linked to the end-Triassic mass extinction. *Proceedings of the National Academy of Sciences* **107**, 6721–5.
- WILLIFORD, K., WARD, P., GARRISON, G. & BUICK, R. 2007. An extended stable organic carbon isotope record across the Triassic-Jurassic boundary in the Queen Charlotte Islands, British Columbia, Canada. *Palaeogeography, Palaeoclimatology, Palaeoecology* **244**, 290–6.
- ZIAJA, J. 2006. Lower Jurassic spores and pollen grains from Odrowąż, Mesozoic margin of the Holy Cross Mountains, Poland. *Acta Palaeobotanica* **46**, 3–83.